



Chloride ions stabilize the glutamate-induced active state of the metabotropic glutamate receptor 3

Amélie S. Tora, Xavier Rovira, Anne-Marinette Cao, Alexandre Cabaye, Linnea Olofsson, Fanny Malhaire, Pauline Scholler, Hayeon Baik, Ann van Eeckhaut, Ilse Smolders, et al.

► To cite this version:

Amélie S. Tora, Xavier Rovira, Anne-Marinette Cao, Alexandre Cabaye, Linnea Olofsson, et al.. Chloride ions stabilize the glutamate-induced active state of the metabotropic glutamate receptor 3. *Neuropharmacology*, 2018, 140, pp.275-286. 10.1016/j.neuropharm.2018.08.011 . hal-02346230

HAL Id: hal-02346230

<https://hal.science/hal-02346230>

Submitted on 13 Feb 2020

HAL is a multi-disciplinary open access archive for the deposit and dissemination of scientific research documents, whether they are published or not. The documents may come from teaching and research institutions in France or abroad, or from public or private research centers.

L'archive ouverte pluridisciplinaire **HAL**, est destinée au dépôt et à la diffusion de documents scientifiques de niveau recherche, publiés ou non, émanant des établissements d'enseignement et de recherche français ou étrangers, des laboratoires publics ou privés.

Chloride ions stabilize the glutamate-induced active state of the metabotropic glutamate receptor 3

Amélie S. Tora^a, Xavier Rovira^{a,e}, Anne-Marinette Cao^b, Alexandre Cabayé^c, Linnéa Olofsson^b, Fanny Malhaire^a, Pauline Scholler^a, Hayeon Baik^a, Ann Van Eeckhaut^d, Ilse Smolders^d, Philippe Rondard^a, Emmanuel Margeat^b, Francine Acher^{c*}, Jean-Philippe Pin^{a*} and Cyril Goudet^{a*}

^a IGF, CNRS, INSERM, Univ. de Montpellier, Montpellier, F - 34094 Montpellier, France

^b Centre de Biochimie Structurale (CBS), INSERM, CNRS, Université de Montpellier, F-34094 Montpellier, France

^c Laboratoire de Chimie et Biochimie Pharmacologiques et Toxicologiques, CNRS UMR8601, Université Paris Descartes, Sorbonne Paris Cité, F-75270 Paris Cedex 6, France

^d Research group Experimental Pharmacology (EFAR/FASC), Center for Neurosciences (C4N), Vrije Universiteit Brussel (VUB), 1090 Brussel, Belgium

^e Present address: Molecular Photopharmacology Research Group, The Tissue Repair and Regeneration Laboratory, University of Vic - Central University of Catalonia, C. de la Laura, 13, 08500 Vic, Spain

*** Corresponding authors:** Cyril Goudet, IGF, 141, rue de la Cardonille, F-34094 Montpellier Cedex 5, France. E-mail: cyril.goudet@igf.cnrs.fr ; Francine Acher, Laboratoire de Chimie et de Biochimie Pharmacologiques et Toxicologiques, CNRS UMR8601, Université Paris Descartes, Sorbonne Paris Cité, 45, rue des Saints-Pères, F-75270 Paris Cedex 6, France. E-mail: francine.acher@parisdescartes.fr ; Jean-Philippe Pin, IGF, 141, rue de la Cardonille, F-34094 Montpellier Cedex 5, France. E-mail: jean-philippe.pin@igf.cnrs.fr

ABSTRACT

Due to the essential roles of glutamate, detection and response to a large range of extracellular concentrations of this excitatory amino acid are necessary for the fine-tuning of brain functions. Metabotropic glutamate receptors (mGluRs) are implicated in shaping the activity of many synapses in the central nervous system. Among the eight mGluR subtypes, there is increasing interest in studying the mGlu₃ receptor which has recently been linked to various diseases, including psychiatric disorders. This receptor displays striking functional properties, with a high and, often, full basal activity, making its study elusive in heterologous systems. Here, we demonstrate that Cl⁻ ions exert strong positive allosteric modulation of glutamate on the mGlu₃ receptor. We have also identified the molecular and structural determinants lying behind this allostery: a unique interactive “chloride-lock” network. Indeed, Cl⁻ ions dramatically stabilize the glutamate-induced active state of the extracellular domain of the mGlu₃ receptor. Thus, the mGlu₃ receptors’ large basal activity does not correspond to a constitutive activity in absence of agonist. Instead, it results mostly from a Cl⁻ mediated amplified response to low ambient glutamate concentrations, such as those measured in cell media. This strong interaction between glutamate and Cl⁻ ions allows the mGlu₃ receptor to sense and efficiently react to sub-micromolar concentrations of glutamate, making it the most sensitive member of mGluR family.

Keywords:

Glutamate; Receptor; Chloride; Constitutive activity; Allostery; GPCR

HIGHLIGHTS

- Chloride ions are strong positive allosteric modulators of mGlu₃ receptor
- A unique “chloride-lock” network dramatically stabilize the active state of the receptor
- This allows the mGlu₃ receptor to sense and react to sub-micromolar concentrations of glutamate

INTRODUCTION

The amino acid L-glutamate is an essential element of life, and has been very early used as a messenger. During evolution, L-glutamate became one of the major neurotransmitters, being the mediator of the neuromuscular junction in arthropods and being responsible for transmitting signals at most fast excitatory synapses in the brain (Fonnum, 1984). Such an essential role of glutamate, associated with all the other functions of this amino acid, imposes a tight regulation of its extracellular concentrations. Indeed, an inaccurate control of extracellular glutamate levels can lead to epilepsy and brain damage through excitotoxicity (Meldrum, 2000). Essential mechanisms have then been selected during evolution to monitor extracellular glutamate concentrations, including active uptake mechanisms and a control of glutamate entry at the level of the blood brain barrier. Defects in these mechanisms have been proposed to be responsible for a number of brain diseases, including neurodegenerative disorders as well as psychiatric diseases or addiction (Kalivas, 2009; Lewerenz and Maher, 2015; Miladinovic et al., 2015).

Glutamate activates cationic glutamate-gated channels (i.e. ionotropic glutamate receptors) that mediate the fast excitatory actions of glutamate. It also activate G protein-coupled receptors, named metabotropic glutamate receptors (mGluRs) (Pin and Bettler, 2016). The eight subtypes of mGluRs are key modulators of transmission at most synapses in the brain. Some mGluRs are located post-synaptically (the group-I mGlu₁ and mGlu₅), allowing a tight control of the post-synaptic response, while others (group-II, mGlu₂ & ₃, and group-III, mGlu₄, ₇ & ₈) are mainly found in pre-synaptic terminals where they inhibit the release of various neurotransmitters. Aside from the group-III mGlu₆, which is responsible of the ON-bipolar neuronal transmission in the retina (Vardi et al., 2000), mGluRs can be considered as glutamate sensors allowing cells to adapt their response as a function of the extracellular glutamate concentration. Indeed, mGluRs are not only found at glutamatergic synapses, but also at other types of synapses, including dopaminergic (DA) and GABAergic synapses, as well as in other regulatory cells such as astrocytes and microglial cells (Nicoletti et al., 2011).

All mGluRs share a common structural architecture (Pin and Bettler, 2016). They are obligate dimers, each protomer being composed of a large bi-lobed extracellular domain (ECD) containing a Venus Flytrap (VFT) and a cysteine-rich domain (CRD) that connects to the seven helices transmembrane spanning domain (TMD). The VFT domain binds orthosteric ligands and also endogenous allosteric modulators, notably extracellular

ions, such as calcium and chloride, that potentiate receptor activity (DiRaddo et al., 2014; Jiang et al., 2014; Kuang and Hampson, 2006; Kubo et al., 1998; Tora et al., 2015; Vafabakhsh et al., 2015).

The group-II mGlu₃ receptor is found at the post-synapse and in pre-synaptic elements in neurons and in astrocytes, facing the micro-vessels, making this receptor a likely key component of the detection of the extracellular glutamate concentration (Mudo et al., 2007; Ohishi et al., 1993; Tamaru et al., 2001). Genetic studies revealed a possible involvement of this receptor in various diseases, including schizophrenia and other psychiatric disorders (Consortium, 2014; De Filippis et al., 2015; Egan et al., 2004; Harrison et al., 2008; O'Brien et al., 2014), as well as cancer development at the periphery (Kunz, 2014; Yi et al., 2017). When compared to other mGlu receptor subtypes, mGlu₃ receptor often displays a strong basal activity in transfected cells, therefore limiting their full functional and pharmacological characterization.

The present study aimed to elucidate the structural and molecular basis of the high basal activity of the mGlu₃ receptor detected in heterologous system, a surprising property given its high structural similarity with the mGlu₂ receptor that does not display the same behavior. We demonstrate the existence of a unique allosteric interaction between glutamate and Cl⁻ ions in the mGlu₃ receptor. This strengthened interaction network increases the stability of the glutamate-induced active state of the extracellular domain of the receptor, making the mGlu3 receptor highly responsive to low ambient glutamate concentrations. Finally, we propose that this mechanism allows an accurate detection of sub-micromolar extracellular glutamate concentrations.

MATERIAL AND METHODS

Cell culture and transfection

HEK293 cells were cultured in Dulbecco's Modified Eagle Medium (DMEM, Life Technologies, Cergy Pontoise, France), supplemented with 10% of Fetal Bovine Serum (FBS) and were transiently transfected with rat mGluRs receptors by electroporation or reverse lipofectamine 2000 protocol as previously described (Doumazane et al., 2013). Receptors were also co-transfected with the glutamate transporter EAAC1 to minimize influence of extracellular glutamate and if needed, chimeric G_i/G_q G-protein (G_qTOP) to allow the coupling to the phospholipase C pathway for second messenger experiments. Cells were seeded in a poly-ornithine coated 96-well plate at the density of 150 000 cells/well. 24h (48h for chimeras) after transfection, medium was changed by Glutamax™ (Life Technologies, Cergy Pontoise, France) to reduce extracellular glutamate concentration 2 hours before experiments.

Directed mutagenesis and chimeras constructs

mGlu₃ mutants receptors were obtained using the Quick-Change strategy (Stratagene, La Jolla, CA, USA). All mutations were made in the HA and HA SNAP encoding plasmids and were verified by sequencing. Total and cell surface expression was quantified by ELISA using anti-HA primary antibody coupled to peroxidase (3F10, Roche, Basel, Switzerland) as previously described (Goudet et al., 2004). For chimeras receptors, a restriction site was introduced after the Venus Flytrap (VFT) encoding sequence in HA SNAP mGlu₂ and mGlu₃ plasmids using the Quick-Change strategy. Then, digested VFT sequences were sub-cloned into mGlu₂ or mGlu₃ plasmids according chimera design and final constructs were also verified by sequencing. Chimeras expression levels were quantified by fluorescence at 620 nm on Lumi4-Tb labeled receptors as described elsewhere (Doumazane et al., 2013).

Chloride buffers composition

All chemical products were purchased from Sigma-Aldrich (L'Isle d'Abeau, France). Reference high Cl⁻ buffer used for calcium mobilization, TR-FRET mGlu sensor and smFRET assays contained 154.6 mM of Cl⁻ ions and included NaCl 150 mM, KCl 2.6 mM, MgSO₄ 1.18 mM, D-glucose 10 mM, HEPES 10 mM, CaCl₂ 1 mM and 0.5% (w/v) BSA. To reach 200 mM Cl⁻ concentration, NaCl was increased. For buffers with lower Cl⁻ concentration, NaCl and KCl were progressively replaced by gluconate equivalents (NaC₆H₁₁O₇ and KC₆H₁₁O₇ respectively). pH was adjusted at 7.4. It was previously shown that gluconate does not impair cell signaling (Tora et al., 2015).

Second messengers assays

Inositol monophosphate production was determined using the IP-One HTRF (Homogenous Time Resolved Fluorescence) kit (Cisbio Bioassays, Codolet, France) according to the manufacturer's recommendations (Trinquet et al., 2006). For the calcium mobilization assay, HA tagged mGluRs expressing cells were seeded in black-walled, clear bottom 96-well plates. High (154.6 mM) and low (2 mM) Cl⁻ buffers supplemented with 4 mM probenecid were used. 24h after transfection, cells were loaded with 1 µM of calcium sensitive fluorescent dye Fluo 4-AM (Life Technologies, Cergy Pontoise, France) diluted in fresh high Cl⁻ buffer, for 1h at 37°C. After washing, cells were maintained in 2 or 154.6 mM Cl⁻ buffers prior glutamate addition. Intracellular calcium release was determined using Flexstation®3 (Molecular Devices, Sunnyvale, CA, USA). Fluorescence was detected for 60 seconds at 485 nm excitation and 525 nm emission. In order to assess gluconate side effects on cell signaling, Ca²⁺ mobilization was also measured after stimulation of an AVP sensitive endogenous receptor on non-transfected cells, which was used as an internal control in each experiment, as previously described (Tora et al., 2015) .

TR-FRET mGlu sensor assay

SNAP tagged mGluRs were used for this assay. Cells were seeded in black-walled, black bottom 96-well plates. 24 hours (48 hours for chimeras) after transfection, receptors were covalently labeled with 100 nM of SNAP-Lumi4-Tb (donor) and 60 nM of SNAP-Green (acceptor) diluted in 154.6 mM high Cl⁻ buffer. Donor and acceptor concentrations were chosen in order to label surface receptors equivalently, with both 1 donor and 1 acceptor molecule. After 1 hour at 37°C, cells were washed in appropriate Cl⁻ buffers and drugs were added. TR-FRET measurements were collected at 520 nm using PHERAstar F5 microplate reader as previously described (Doumazane et al., 2013).

Data analysis

IP-One, Ca²⁺ mobilization and TR-FRET data were analyzed with Prism 6 software (GraphPadSoftware, San Diego, CA, USA). Concentration-responses curve parameters were derived using a four-parameter non-linear regression equation. For clarity, potency was expressed as absolute (positive) logarithms (pEC₅₀) and nH (Hill slope) describes the steepness of the curve. In Cl⁻ experiments, data from Ca²⁺ mobilization were normalized by the WT receptor maximum response obtained in 2 mM Cl⁻ buffer and E_{max} represent the maximum response obtained at saturating agonist concentration. In TR-FRET mGlu sensor assay, base and maximum of the curve were normalized by high and low FRET ratio of the WT receptor in 2 mM Cl⁻ buffer to define respectively 100% and 0% of the signal. For chimeras experiments, data were normalized by mGlu₂ receptor maximum window (top and bottom of mGlu₂ receptor curve). Data shown in the figures represent the mean ± S.E.M. of at least three experiments performed at least in duplicates. Statistical differences were determined by One-way ANOVA with Dunnett's and Sidak's post-test.

smFRET experiments

For smFRET experiments, human SNAP tagged mGluRs extracellular domains (ECD) fused to a GPI anchor in the C-terminus (HA SNAP mGlu₃ Del570 GPI) were transiently co-transfected with glutamate transporter EAAC1 in HEK293 TSA cells by reverse Lipofectamine 200 protocol (Life Technologies, Cergy Pontoise, France), in 6-well plates. After 24 hours expression, receptors were covalently labeled with 100 nM Benzyl-Guanine-Cy3B (donor) and 1 µM Benzyl-Guanine-d2 (acceptor) (Cisbio Bioassays, Codolet, France) diluted in fresh 154.6 mM high Cl⁻ buffer for 1 hour at 37°C. Then several washings with different Cl⁻ buffers were performed prior to ECD cleavage using 0.25 U.ml⁻¹ *Bacillus cereus* Phosphatidylinositol-specific Phospholipase C (Life Technologies, Cergy Pontoise, France), at 37°C for 30 minutes. ECD were purified using Zeba™ spin desalting columns (Life Technologies, Cergy Pontoise, France) and stored at -20°C supplemented with 50% glycerol and 0.1 mg.ml⁻¹ BSA. For smFRET measurements, samples were diluted to picomolar concentration and loaded into 384-well plates (Greiner Bio One). Data acquisition was performed on our home-built confocal MFD-PIE (Multiparameter Fluorescence Detection – Pulsed Interleaved Excitation) microscope (Olofsson and Margeat, 2013) as previously described (Olofsson et al., 2014). Data analysis was performed using the Software Package for Multiparameter Fluorescence Spectroscopy, Full Correlation and Multiparameter Fluorescence Imaging developed in C.A.M. Seidel lab (<http://www.mpc.uni-duesseldorf.de/seidel/>)(Widengren et al., 2006). Pulsed interleaved excitation allowed us to construct the 2D-histogram of the proximity ratio E_{PR} (i.e. FRET efficiency) and stoichiometry ratio S, where single-labeled species and/or free fluorophores can be excluded, and only double-labeled species are selected for further analysis. Apparent E_{PR} histograms were analyzed using Origin® 8. At least three measurements were performed for each sample and data shown in the figures represent the mean ± S.E.M. Statistical differences were determined by One-way ANOVA with Sidak's post-test.

Binding assay

For ligand binding assay, membranes from mGluRs transfected HEK293 cells were prepared. After 48 hours expression, cells were washed with cold PBS, scratched and collected by centrifugation at 4°C. Then

membranes were prepared by successive homogenization (on ice) and centrifugation (1000 rpm at 4°C) steps. After a final centrifugation at 19 500 rpm for 2 hours at 4°C, membranes were resuspended in sensor buffer (high Cl⁻), quantified by BCA method and stored at -80°C. For binding assay, 15-20 µg of mGlu₂ or mGlu₃ membranes were incubated respectively with 5 or 3 nM [³H]-LY341495 (corresponding to Kd of this radioligand) and various concentrations of cold glutamate for 1h at room temperature. Membranes were then collected on filters and washed 3 times with a 0.9% NaCl solution. Filters were placed in tubes containing a liquid scintillation mixture solution, and radioactivity was measured with a Packard beta counter (Perkin Elmer). Unspecific binding was determined in presence of 100 µM LY379268. Data were analyzed with Prism 6 software (GraphPadSoftware, San Diego, CA, USA) to determine Ki values.

Glutamate quantification

Medium from plated cells transiently expressing mGluRs with or without EAAC1 transporter was sampled for glutamate analysis at different experiment times: after 24 hours expression, cells were washed one time and let 15 min in sensor assay buffer (high Cl⁻); then 2 hours or 5 hours after medium change by Glutamax™. Glutamax™ medium, IP-One and high Cl⁻ Ca⁺/sensor assay buffers were also tested. Samples were filtered on 0.2-0.8 µm filters prior to analysis.

Glutamate quantification was performed by a reversed phase narrow bore liquid chromatography assay with fluorescence detection after precolumn derivatization with o-phtalaldehyde and β-mercaptoethanol, as previously described (Van Hemelrijck et al., 2005). The compounds were eluted by gradient elution with a mobile phase that was delivered at a rate of 0.17 mL/min. The gradient elution was performed using mobile phase A (0.025 M sodium phosphate solution pH 9 and 1% tetrahydrofuran) and mobile phase B (methanol:water 90:10). The temperature of the autosampler tray was set at 4°C and the injection volume was 10 µL on a C18 narrow bore column (5 µm particle size, 250 x 2 mm, Capcell Pak MG®, Shiseido). Detection was performed with a RF 10A XL fluorescence detector (Shimadzu) at excitation and emission wavelengths of 340 and 450 nm, respectively. Data acquisition was carried out with the integration computer program Clarity (DataApex, Antec, Zoeterwoude, the Netherlands). All analyses were performed at least in duplicate.

Structural and sequence analysis

Crystal structures of mGlu₂ (PDB 4XAQ) and mGlu₃ receptors (PDB 5CNK, 2E4U) were used to compare their VFT domains using the Discovery Studio 4.0 software (BIOVIA – A Dassault Systèmes brand – 5005 Wateridge Vista Drive, San Diego, CA 92121 USA). For multiple sequence alignment, we used Discovery Studio's tool Align123 based on the ClustalW program (Thompson et al., 1994). Sequences were obtained from Uniprot website (<http://www.uniprot.org/>), using the gene names for the queries, and only the sequence of the extra-cellular domain (ECD) was kept for the alignment. Output alignment was then further optimized.

RESULTS

The glutamate binding domain is involved in the high basal activity of the mGlu₃ receptor

First, we compared the glutamate-induced production of second messengers by the different mGluRs. Receptors were transiently transfected in HEK293 cells and their glutamate-induced signaling responses were evaluated by measuring inositol monophosphate (IP1) production (**Fig.1A**). To allow the G_i-coupled group-II and -III mGluRs to activate the phosphoinositides pathway, receptors were co-transfected with a G_i/G_q chimeric G-protein. We found that the basal IP1 production was very high in mGlu₃-expressing cells, in contrast to cells expressing other mGluR subtypes ($p < 0.001$), such that glutamate addition did not induce a significant increase of IP1 production.

To understand the structural origin of this phenomenon, we compared the activity of the mGlu₃ receptor to its closest relative mGlu₂ and built mGlu_{2/3} receptor chimeras by inverting their VFT domains. We then measured their activity using both functional (IP1 production) and conformational mGluR sensors (**Fig.1B-C, supplemental figure 1 and supplemental table 1**). These latter are based on VFT conformational changes occurring during receptor activation. SNAP-tags are inserted at the N-termini of each mGluR subunit and are covalently labeled with fluorescent dyes. Variation in distance between the fluorophores can be measured using Lanthanide Resonance Energy Transfer (LRET), using a Time-Resolved Förster Energy Transfer approach (TR-FRET) (Doumazane et al., 2013; Scholler et al., 2017). Agonist binding induces closure of mGluRs VFT domains, leading to a reorientation of the protomers increasing the distance between the N-termini and so, resulting to a large decrease in the TR-FRET signals (**Fig.1D**).

In contrast to what was observed with the mGlu₂ receptor, glutamate concentration-response curves from mGlu₃ receptor-expressing cells were nearly flat in both the IP1 and TR-FRET assays (**Fig.1B-C**). In vehicle conditions, the low FRET ratio measured for mGlu₃ receptors suggested most receptors were mainly in an active conformation, despite the lack of glutamate addition (**Fig.1C, supplemental table 1**). This result, combined with high IP1 levels in the same condition, highlights the high basal activity of mGlu₃ receptors.

When mGlu₂ VFT was fused to mGlu₃ TMD (VFT2/TMD3 chimera), this basal activity was abolished and the receptor could be activated by glutamate similarly to the mGlu₂ receptor. In contrast, the fusion of mGlu₃ VFT with mGlu₂ TMD (VFT3/TMD2 chimera) showed an enhanced basal activity and a nearly flat glutamate concentration-response curve, similar to the mGlu₃ receptor (**Fig.1B-C, supplemental table 1**). Taken together, these findings revealed that mGlu₃ VFT domain plays a key role in the high basal activity of the receptor.

Glutamate is required for the mGlu₃ receptor high basal activity

To explore the potential involvement of glutamate in the high basal activity of mGlu₃ receptors, we first measured conformational changes in presence or absence of the competitive antagonist LY341495 (**Fig.2A**). Interestingly, in presence of LY341495, the FRET ratio is significantly increased ($p<0.001$) in comparison to the ratio measured in the vehicle condition. These results suggest either that LY341495 is an inverse agonist, or that possibly it competes with ambient glutamate present in the assay medium, preventing its action on the receptor.

We then designed a mutant mGlu₃ receptor less sensitive to glutamate. To that aim, we mutated the threonine in position 174, a key residue involved in the binding of the amino acid moiety of glutamate (Acher and Bertrand, 2005), into an alanine. We then measured the conformational changes of mGlu₃ T174A in comparison to the WT mGlu₃ receptor. As expected, the mGlu₃ T174A construct was not activated by glutamate, except at high concentrations (1 mM) where a small decrease in the FRET ratio was measured. Interestingly, contrary to WT receptor, the mGlu₃ T174A mutant did not display any basal activity (**Fig. 2B**). Decreasing receptor affinity for glutamate strongly reduces its basal activity, further supporting a key role of ambient glutamate provided by the cells in such an assay.

We quantified the ambient glutamate concentrations in cell media and buffers used for our experiments (**table 1**). The glutamate concentration in cell medium is strongly affected by incubation time after transfection and co-expression of high-affinity glutamate transporter EAAC1. In optimized experimental conditions (i.e.

EAAC1 co-expression and 2 hours incubation in a glutamate-free cell medium before experiments, see Material and Methods section for details), a residual glutamate concentration of $0.59 \pm 0.03 \mu\text{M}$ was measured.

To correlate this result to glutamate affinity, we performed binding experiments on mGlu₂ and mGlu₃ receptors expressing membranes (**supplemental Fig.2**). Radiolabeled LY341495 displacement curves indicated that the mGlu₃ receptor has a higher affinity for glutamate (sub-micromolar range, $0.90 \pm 0.31 \mu\text{M}$) compared to its homolog mGlu₂ receptor (ten micromolar range, $10.95 \pm 6.92 \mu\text{M}$). Of note, the glutamate Ki value of the mGlu₃ receptor calculated from binding experiments correlated to the extrapolated potency derived from conformational sensor experiments in **Fig.3** (0.88 vs. $0.90 \mu\text{M}$) (**supplemental table 2**). According to the glutamate concentration in the assay, we can deduce that about 40% of the receptors are occupied in these conditions.

Altogether, these results are highlighting that high basal activity likely of the mGlu₃ receptor results mainly from receptor activation by ambient glutamate.

Extracellular chloride modulates both basal and agonist-induced mGlu₃ receptor activity

We have previously reported the positive allosteric modulation of mGluRs' activity by Cl⁻ (Tora et al., 2015), with the mGlu₂ receptor being the less sensitive to extracellular Cl⁻ as compared to other mGluRs. In that study, the effect of Cl⁻ on mGlu₃ receptor was not considered. However, another study proposed that Cl⁻ ions could directly activate mGlu₃ receptor (DiRaddo et al., 2015). In the light of these findings, we thus examined the effect of extracellular Cl⁻ on mGlu₃ receptor basal and agonist-induced activity.

First, the receptor activity was measured both by functional (intracellular Ca²⁺ mobilization) and conformational assays (TR-FRET mGlu sensor assay) in two different buffers containing either a physiological (154.6 mM, referred to "high Cl⁻") or a low Cl⁻ concentration (2 mM, referred to "low Cl⁻"), where Cl⁻ ions were replaced by gluconate equivalents to maintain osmolarity. In the functional assay, the glutamate concentration-response curve of mGlu₃ was nearly flat in high Cl⁻ buffer, whereas a robust dose-dependent activation of mGlu₃ receptors by glutamate can be observed in the low Cl⁻ buffer (**Supplemental Fig.3**

supplemental table 2). In the conformational assay, a concentration-dependent change of FRET signal was observed in both high and low Cl⁻ buffers (**Fig.3A**). However, in the basal condition, the TR-FRET ratio in the high Cl⁻ buffer is approximately half of the ratio observed in the low Cl⁻ buffer (**Fig.3A, supplemental table 2**).

Positive cooperativity between Cl⁻ and glutamate is further highlighted in **figure 3B**. Increasing extracellular Cl⁻ concentration potentiated both receptor basal activity and glutamate potency, in a concentration-dependent manner. To quantify the Cl⁻ effect, we plotted FRET ratios from **Fig.3B** to define a Cl⁻ concentration-response curve either in vehicle condition or in presence of 30 μM of glutamate (the latter corresponds to a concentration engendering 80 % of the maximal response (i.e. EC₈₀), in high Cl⁻) (**Fig.3C**). At EC₈₀, Cl⁻ potency was estimated to 30.98 mM, indicating a strong positive modulation on mGlu₃ receptors. The Hill slope value was 1.11 ± 0.24, suggesting Cl⁻ effect may occur predominantly at one binding site. Interestingly, in absence of glutamate addition, Cl⁻ concentration-response curve was not well defined, but Cl⁻ potency could be extrapolated to 470.10 mM, a concentration far above the physiological range which is considered to be around 120 mM (Jiang et al., 1992). Taken together, these findings indicate mGlu₃ receptor is highly modulated by Cl⁻, in contrast to its homolog mGlu₂ (**Fig.3D**).

We then measured conformational changes in presence or absence of the competitive antagonist LY341495 in low and high Cl⁻ buffers (**Fig.3E**). Interestingly, contrary to what is observed in high Cl⁻ buffer (**Fig.2A**), LY341495 did not change the FRET ratio in low Cl⁻ buffer as compared to the vehicle condition. These results suggest that reducing the mGlu₃ receptor affinity for glutamate by depleting extracellular Cl⁻ dramatically decreases its basal activity, in line with the results obtained with the insensitive mutant mGlu₃ T174A receptor.

Taken together, these results highlight the link between extracellular Cl⁻ concentration, glutamate and the mGlu₃ receptor's basal activity. They suggest that the high basal activity of the mGlu₃ receptor may result from Cl⁻ potentiation of the activity induced by residual glutamate.

Chloride ions favor agonist-induced conformational change of the mGlu₃ receptor

To better understand the consequence of Cl^- modulation on the receptor, we further analyzed the glutamate-induced conformational changes at the single molecule (smFRET) level in comparison to the ensemble level (TR-FRET) (**Fig.4**).

Compared to ensemble FRET, smFRET allows the measurement of sub-millisecond conformational dynamics, thus providing a more accurate analysis of receptor activation mechanisms (Olofsson et al., 2014). We used isolated SNAP-tagged mGlu₃ extracellular domains (ECD) for smFRET experiments, as previously described for mGlu₂ receptors (Olofsson et al., 2014). This glycosylphosphatidyl inositol (GPI)-fused construct is cleaved by phospholipase C (PLC) in order to produce soluble ECDs, labeled with smFRET compatible fluorophores (**Fig.4B, upper panel**). Like full-length receptors, soluble ECDs oscillate between an active and an inactive state. This conformational equilibrium is affected by ligand binding, therefore shifting the apparent FRET efficiency (E_{PR}) of the main population in smFRET experiment on diffusing molecules (**Fig.4B, lower panel**). Moreover, the use of highly diluted solutions of purified ECDs allows working with solutions containing very low ambient glutamate concentrations.

We tested the effect of Cl^- concentrations (2, 75 and 154.6 mM) on basal conditions (vehicle) or following glutamate addition on WT mGlu₃ receptor or on mGlu₃ T174A mutant, which is less sensitive to glutamate. Both TR-FRET and smFRET data confirmed the effect of Cl^- on the equilibrium shift of the WT receptor dimer toward the active state, as seen both on basal activity (vehicle condition) and glutamate-induced FRET changes. In contrast, we observed that mGlu₃ T174A is not activated by glutamate, as expected, nor by Cl^- (**Fig.4A and C, supplemental Fig.4**). Therefore, the Cl^- ion appears as a strong positive allosteric modulator of the mGlu₃ receptor but did not display agonism by itself. Taking together, these results further confirm that the basal activity of mGlu₃ is due to the receptor's high affinity for glutamate and Cl^- potentiation of glutamate binding.

A unique “chloride lock” stabilizes the active state of the mGlu₃ receptor

To delineate a molecular basis of the mGlu₃ receptor's Cl⁻-related basal activity, we examined the crystal structures of mGlu₃ and mGlu₂ VFTs (PDB 5CNK and 4XAQ, respectively), recently solved in their dimer active closed conformation (Acc) binding the potent agonist LY354740 and glutamate (Glu) respectively (Monn et al., 2015a; Monn et al., 2015b) (**Fig.5**).

A first difference resides in the number of Cl⁻ binding sites in mGlu₂ and mGlu₃ VFTs. Several halide sites can be observed in mGlu₃ VFT (**Figure 5A-B**). Among them, two sites correspond to functional Cl⁻ binding sites that have been described in the VFT of most mGluRs, contrary to the mGlu₂ receptor, which possesses only one of these functional sites (Tora et al., 2015). The first Cl⁻ site (Site 1) is located within VFT lobe 1, in a binding pocket adjacent to the glutamate binding site, which was previously predicted (Acher et al., 2011) and demonstrated to be a Cl⁻ binding site conserved in all mGluRs (**Supplemental Fig.6A**) (DiRaddo et al., 2015; Tora et al., 2015). The second site (Site 2) is created by the interface of both VFT lobes, when the receptor is in a closed active conformation and shows more divergence within the mGluR family. This binding site is absent in mGlu₂ where the S152 that is critical for Cl⁻ binding in site 2 is replaced by an aspartate residue (Tora et al., 2015).

Another major difference between mGlu₂ and mGlu₃ VFT appears at α -helix 7 and loop 7 (**Fig.5A-B and supplemental Fig. 6**). Whereas loop 7 adopts a straight conformation in mGlu₂, it is longer and curled in mGlu₃ because of α -helix 7 unfolding. This occurrence results in a critical difference at the dimer interface between the Acc protomers, which allows several additional interactions with the facing monomer. A closer look at the mGlu₃ structures suggests that Cl⁻ bound at site 2 could coordinate this network of interactions between the two lobes, tightening the closed VFT. In particular, Cl⁻ may bridge S152 (lobe 1, loop 3) and R277 (lobe 2, loop 8) in the agonist-induced closed VFT conformation (**Fig. 5C-D right panel**). Due to the ionic nature of the chloride, the interaction between S152 and R277 is stronger compared to that with a neutral water molecule (Rozas et al., 2008) (**Fig. 5D central and right panel**). Thereby, Cl⁻ may act as a "Cl⁻ lock" underlying the high agonist affinity by stabilizing the glutamate-induced closed conformation of mGlu₃ VFT (Fig. 5 and 6).

To verify our hypothesis, we mutated mGlu₃ S152 that seems to be crucial in Cl⁻ binding into an aspartate (as in mGlu₂) or an alanine and measured receptor activation by TR-FRET assay and signaling activity by Ca²⁺

mobilization (**Fig.5E**, **supplemental Fig.6B-D and supplemental table 2**). Glutamate potencies of mGlu₃ S152A and mGlu₃ S152D were not changed compared to the WT receptor in high Cl⁻ buffer (**supplemental Fig.6B**). However, both S152A and S152D mutations abolished the receptor's basal activity. Indeed, FRET ratios measured in high Cl⁻ were similar to the WT receptor in low Cl⁻ (**Fig.7C**). Ca²⁺ mobilization data indicated signaling activity was rescued for both mutants in high Cl⁻ buffer, in comparison to the WT (**supplemental Fig.6C**). Regarding Cl⁻ sensitivity, the mGlu₃ S152D mutant exhibited a reduced Cl⁻ sensitivity, similar to the mGlu₂ receptor (**supplemental table 2**). Mutations did not change expression of the receptor (**supplemental Fig.6D**). Taken together, these data confirmed the involvement of Cl⁻ binding site 2 in mGlu₃ receptor's activity and unravel the key role of S152 on ion stabilization.

At a molecular level, these data may be interpreted in terms of stability of the active conformation of the receptor. With the mutants S152D and S152A of the mGlu₃ receptor, the most stable network is similar to that at low Cl⁻ concentrations and the high basal activity is thus not observed, resembling to what happens at mGlu₂ receptors.

DISCUSSION

In this study, we investigated the molecular mechanisms underlying the atypical high-basal activity observed in cells expressing the mGlu₃ receptor. Our main finding shows that it is not corresponding to a constitutive activity of the mGlu₃ receptor in the absence of bound agonist. Instead, it results mostly from a Cl⁻-mediated amplified response to low ambient glutamate concentrations, such as those measured in cell media. This strong positive allosteric modulation of glutamate by Cl⁻ ions allows the mGlu₃ receptor to sense and efficiently react to sub-micromolar concentrations of glutamate, making it the most sensitive member of mGluR family.

Ion dependence of mGluRs activity has been previously reported, notably to Ca²⁺ and Cl⁻ (Kuang and Hampson, 2006). While mGlu₁ and mGlu₃ receptors were demonstrated to be sensitive to Ca²⁺, Cl⁻ modulation was reported for all mGluRs, with a lesser extent for the mGlu₂ receptor (DiRaddo et al., 2014; Jiang et al., 2014; Tora et al., 2015; Vafabakhsh et al., 2015). Of note, the cooperativity between an amino acid ligand and ions to stabilize the active conformation of the receptor is also observed in another receptor from the GPCR class C, the Ca²⁺ sensing receptor. This receptor is activated concomitantly both by Ca²⁺ ions and an L-amino acid, such as L-Phe, that binds in a pocket corresponding to the glutamate binding pocket in mGluRs (Zhang et al., 2014). Here, we showed that the mGlu₃ receptor is particularly strongly potentiated by Cl⁻ ions as compared to other mGluRs. This strong positive cooperativity between Cl⁻ ions and glutamate occurs through a unique strengthened interaction network between the two lobes of the extracellular domain of the mGlu₃ receptor. This network acts as a “Cl⁻-lock” that dramatically reinforces glutamate binding and function. Previously, both Ca²⁺ and Cl⁻ ions were proposed to display agonist activity on the mGlu₃ receptor (DiRaddo et al., 2015; Vafabakhsh et al., 2015). However, in our experiments, Cl⁻ *per se* does not display direct agonism, as revealed by the glutamate insensitive mGlu₃ mutant T174A, which is not activated by Cl⁻. We propose that what has been interpreted previously as Cl⁻ direct agonism in very sensitive assays may correspond in fact to the potentiation by Cl⁻ ions of the activity induced by residual ambient glutamate. Indeed, cells are constitutively releasing glutamate in extracellular media. We have recorded concentrations ranging from 0.6 to more than 5 μM. These glutamate concentrations are in line with those measured in another recent

publication (Doornbos et al., 2018). Thus, Cl⁻ ions are pure positive allosteric modulators of the mGlu₃ receptor.

It is unlikely to observe the occurrence of rapid Cl⁻ concentration changes compatible with dynamic modulation of mGlu₃ receptor activity. Short-term variations occur during transport or synaptic activities where rapid Cl⁻ fluxes through GABA or glycine-gated ion channels modify Cl⁻ concentrations (Staley et al., 1995). We have previously evaluated the discrete variations of Cl⁻ concentrations in the synaptic cleft during GABAergic events in physiological or pathological conditions (Tora et al., 2015). We found that multiple synaptic events can modify synaptic Cl⁻ concentrations up to 25 mM. Long-term changes in Cl⁻ concentrations can be observed during maturation (Ben-Ari et al., 2007), modifications of extracellular matrix (ECM) and pathologies (De Koninck, 2007; Kaila et al., 2014). Interestingly, fast extracellular Cl⁻ changes due to synaptic activity and slow changes could be additive. Thus, in particular conditions, such as anoxia where variations of Cl⁻ exceeding 30 mM can be observed (Jiang et al., 1992), Cl⁻ variations could reach up to 55 mM. However, given the potency of Cl⁻ on the mGlu₃ receptor (~30 mM) as compared to the physiological extracellular Cl⁻ concentration in mature CNS (~120 mM), the potentiation of mGlu₃ receptor activity by Cl⁻ ions is probably mostly constitutive. Other members of the mGluR family could be dynamically regulated by Cl⁻, such as the presynaptic mGlu₄ receptor (Tora et al., 2015). Indeed, unlike the mGlu₃ receptor, mGlu₄ presents characteristics that make it more susceptible to be actively regulated by discrete Cl⁻ variations. First, this receptor is expressed in GABAergic synapses where rapid Cl⁻ variations occur following opening of GABA_A receptors. Second, the potency of Cl⁻ on mGlu₄ receptor is close to the physiological Cl⁻ concentration (~80 mM) and presents a steep relationship between Cl⁻ and glutamate-induced activity (with an N_{Hill} ~6). This means that small changes in Cl⁻ concentration yield to large changes in response to glutamate. On the other hand, dramatic changes in Cl⁻ homeostasis occur during CNS maturation (Ben-Ari et al., 2007). We can hypothesize that mGlu₃ receptors should shift from a “dynamic” mode of glutamate response during the early stages to the highly-glutamate sensitive and sustained response mode described in the present study in mature stages. This should affect its biological functions in early stages, such as the crucial control of mGlu₅-mediated neuroprotection described in Di Menna et al. (Di Menna et al., 2018). One can hypothesize that when extracellular Cl⁻ concentrations are low in premature stages, mGlu₃ receptor should be able to signal and regulate the release of neurotrophic factors from astrocytes, given its high Cl⁻ sensitivity. However, in the

absence of specific data this remains purely speculative and further investigations will be needed to evaluate the impact of Cl⁻ on mGluR function in the premature brain. In the mature brain, while it is unlikely to observe the occurrence of Cl⁻ concentrations changes compatible with a significant modulation of mGlu₃ receptor activity, a Cl⁻ mediated rapid adaptation of the regulatory role of some mGluRs, such as mGlu₄ receptors present on GABAergic terminals, could be observed.

Although the overall structures of mGlu₂ and mGlu₃ VFTs are highly similar, two major differences can be observed: (i) the number of functional Cl⁻ binding sites, one in mGlu₂ versus two in mGlu₃ receptors and (ii) the loop 7 in lobe 2 is longer in mGlu₃ than in the mGlu₂ receptor. These two particularities of the mGlu₃ receptor contribute to the building-up of a unique “Cl⁻ lock” that greatly stabilizes the glutamate-induced closed conformation of its VFT. Indeed, as compared to mGlu₂, the presence of Cl⁻ in site 2 in mGlu₃ receptor is coordinating a network of interactions between the two lobes, involving notably the twisted loop 7, that is tightening the closed VFT. As a result, the atypical high-basal activity of the mGlu₃ receptor is not observed in the cognate mGlu₂ receptor in which the Cl⁻ lock is absent. The residue S152 seems to play a crucial role in Cl⁻ binding and bridging between the lobes. This amino acid was previously reported to be involved in mGlu₃ Ca²⁺-based basal activity (Kubo et al., 1998; Vafabakhsh et al., 2015), but no Ca²⁺ ion was found in crystal structures at this location. Regarding literature, Ca²⁺ seems to play a role in mGlu₃ receptor activity, but its binding(s) site(s) as well as its contribution to the receptor’s basal activity remains unclear. In contrast, in the mGlu₂ receptor, the corresponding serine residue is mutated into an aspartate (D146), which disrupts Cl⁻ binding at site 2, explaining divergence with mGlu₃ receptors towards both Cl⁻ sensitivity and basal activity. Prior to this study, D146 has been proposed to disrupt the cation-pi interaction and also the Cl⁻ binding site 1, by engendering a flip of R271 (so called “arginine flip”), thus postulating there would be no Cl⁻ binding sites in mGlu₂ (DiRaddo et al., 2015). However, in recently released mGlu₂ VFT crystal structure (Monn et al., 2015b), the cation-pi interaction is intact and only one Cl⁻ ion is found in site 1, which is consistent with our previous study and the present data (Tora et al., 2015). In addition, it is worth to mention that another Cl⁻ ion is localized near the cation-pi in this structure, but at a different site from site 2, as it is found in only one protomer and therefore may be a crystallization artefact. Additional inter-lobe connections may also participate to the closed VFT stabilization, such as R249 (lobe 2, loop 7), which can bind to G51 (lobe 1, loop 1) in mGlu₃ receptors because of the unfolding of the α-helix 7 and a new conformation of loop 7 (Fig. 5C and D right).

panels). The H-bond between R249 and G51 carbonyl is weaker than the salt bridge with D102 that occurs in mGlu₂ (Fig.5C and D left panels), nevertheless this loss of stability is compensated by new interactions at the dimer interface between loop 7 and helix 6 of the other monomer (**See Fig. 6 and supplemental Fig. 5**). This interaction network could possibly explain why the two mGlu₃ VFT monomers are closer than those of mGlu₂. One can speculate that this proximity may further increase the stability of the active dimer resulting in the basal activity of the receptor at low glutamate concentrations. However, further studies will be necessary to determine more precisely the dimer interface and its involvement in receptor activation.

The specific pathophysiological roles of the mGlu₃ receptor are still poorly understood. Until recently, these studies have been hampered by the lack of selective tools discriminating between the cognate mGlu₂ and mGlu₃ receptors. Indeed, the orthosteric binding sites of these two receptors are 100% identical, making the identification of selective orthosteric ligands highly challenging. Thus, the first ligands available were selective for the group II mGluRs over other groups, but failed to discriminate between mGlu₂ and mGlu₃ receptors (Celanire et al., 2015). Still, mGlu_{2/3} ligands have been very helpful to highlight the involvement and the therapeutic potential of these receptors in different CNS disorders, notably in anxiety, schizophrenia, addiction, depression and chronic pain. Recently, several selective mGlu₃ negative allosteric modulators (Engers et al., 2015) or orthosteric ligands (Monn et al., 2018; Monn et al., 2015b) have been identified. The selectivity of these newly discovered orthosteric ligands lies behind their interaction with amino acids residing at the periphery of the glutamate binding site of the mGlu₃ receptor (Monn et al., 2018). Indeed the crystal structure of LY2794193, a selective mGlu₃ agonist, bound to mGlu₃ VFT (PDB ID 6B7H) reveals that its methoxyphenyl substituent pushes away R277 but does not prevent the stabilization of the active dimer with the curled loop7 (**Supplemental Fig. 7**) (Monn et al 2018). On the other hand, a similar perturbation of R271 in mGlu₂ decreases significantly the receptor activation. Thus, it appears that targeting the Cl⁻ binding sites of mGlu₃ receptor provide an interesting way to overcome the difficulty of designing selective orthosteric drugs. Interestingly, this approach is also valid for other mGluRs. For example, the first mGlu₄ receptor selective orthosteric agonist named LSP4-2022 is a dualsteric/bitopic ligand targeting both the glutamate- and the Cl⁻ binding pockets of the mGlu₄ receptor (Goudet et al., 2012; Selvam et al., 2018). Hopefully, new selective ligands will help to better define the particular roles of mGlu₃ receptors.

Interestingly, mGlu₂ and mGlu₃ receptors differ notably by their cellular distribution. Whereas mGlu₂ receptors are mostly neuronal, mGlu₃ receptors are expressed both in glia and in neurons. In neurons, mGlu₃ receptors are present at the post-synapse and in presynaptic elements (Tamaru et al., 2001) where their activation reduces synaptic activity and plasticity (Harrison et al., 2008). Interestingly, a functional partnership between neuronal mGlu₃ receptors and mGlu₅ receptors has recently been described, in which activation of mGlu₃ receptors amplifies mGlu₅ receptor signaling and shapes the ability of mGlu₅ receptors to either amplify or restrain neuronal toxicity (Di Menna et al., 2018). In astrocytes, mGlu₃ receptors have been shown to regulate important functions such as the release of astrocytic glutamate and other factors (Aronica et al., 2005; Corti et al., 2007; Nicoletti et al., 2015), the re-uptake of glutamate (Aronica et al., 2003), nitrate homeostasis (Wang et al., 2016) and are involved in neuroprotection (Battaglia et al., 2015; Corti et al., 2007). By promoting glutamate sensing in the extracellular space, through the molecular mechanisms described in this study, the mGlu₃ receptor could react effectively to concentrations of glutamate below the micromolar range. This might confer mGlu₃ receptor the ability to regulate the basal tone of glutamate release from neuronal presynaptic elements, as well as basal release of neuroprotective factors, thereby participating to the fine regulation of glutamate reuptake by glia.

Given the numerous physiological and pathological actions of glutamate, it is crucial to control acutely extracellular glutamate concentrations in the brain. Indeed glutamate becomes neurotoxic at elevated extracellular concentrations and glutamate dysregulation is associated to many CNS disorders. Different actors ensure the control of glutamate homeostasis. Transporters are maintaining low concentrations of synaptic and extrasynaptic glutamate. While ionotropic glutamate receptors are responsible of the fast-synaptic response to glutamate, mGluRs are responsible for its slow neuromodulatory actions. Group I mGluRs positively modulate responses to glutamate while group II and group III receptors are decreasing neuronal activity by downregulating the release of neurotransmitters. Interestingly, the eight members of the mGluR family display different affinities for glutamate. Three members present submicromolar affinity for glutamate: mGlu₁ with 0.3 μM (Mutel et al., 2000; Thomsen et al., 1993), mGlu₅ with 0.5 μM (Mutel et al., 2000) and mGlu₃ which Ki values range from 0.041 to 0.9 μM (Johnson et al., 1999; Laurie et al., 1995; Schweitzer et al., 2000) and 0.9 μM in the present study. While the mGlu₃ receptor affinity for glutamate is in the same range than the ones of mGlu₁ or mGlu₅ receptors, its relatively high glutamate affinity combined to its unique Cl⁻ lock favoring the

agonist-induced state makes the mGlu₃ receptor able to sense and fully respond to submicromolar glutamate concentrations. This could enable mGlu₃ receptors to play a role in the regulation of basal conditions with low tone of glutamate. Other members of the family, mGlu_{2, 4, 6 and 8} receptors present intermediate affinities, in the micromolar range, for glutamate, (Cartmell et al., 1998; Eriksen and Thomsen, 1995; Schweitzer et al., 2000; Wright et al., 2000). On the opposite side of the spectrum, the mGlu₇ receptor is activated by millimolar concentrations of glutamate, with an affinity around 900 μM (Wright et al., 2000). This receptor is located in the synaptic grid where glutamate is released and can reach occasionally such high concentrations. Contrary to mGlu₃ receptor, the role of mGlu₇ receptor would then be to react to the highest concentrations of glutamate and may ensure a role of safety valve. This mGluRs large spectrum of glutamate sensitivity associated to their widespread synaptic, non-synaptic and glial distribution allows them to participate to a fine neuroadaptation of the CNS.

In conclusion, we demonstrated that the atypical high-basal activity of the mGlu₃ receptor results mostly from its activation by low ambient glutamate concentrations. This is due to a unique interaction network located in the extracellular domain of the mGlu₃ receptor. This network acts as “Cl⁻ lock” that is strongly stabilizing the glutamate-induced active conformation of the receptors. This strong allosteric control of the mGlu₃ receptor by physiological Cl⁻ ions allows it to sense and respond efficiently to low concentrations of glutamate. Thus, the various mGluR subtypes appear as a family of glutamate sensors able to respond to a wide range of conditions, from high nanomolar to millimolar concentrations of glutamate. Among them, mGlu₃ receptor is the most sensitive member of this family, able to mediate sustained responses to low tone of glutamate.

ACKNOWLEDGMENTS

The authors thank Ebba L. Lagerqvist for critical reading of the manuscript. This work was supported by grants from the Fondation Recherche Médicale (FRM team DEQ20130326522 and DEQ20170336747) to JPP, the Fundació La Marató de TV3 (Ref 110232), Eranet Neuron, the Agence Nationale de la Recherche (ANR-12-NEUR-0003, ANR-13-BSV1-006 to CG, ANR-09-BIOT-018 to JPP and ANR-13-BSV5-0007 to PR) and “Chercheur d'Avenir” grant from the Region Languedoc Roussillon to EM. Cell-based pharmacological assays were performed on the ARPEGE (Pharmacology Screening-Interactome) platform facility at the IGF. JP Pin's research group belongs to the Labex EpiGenMed (ANR-10-LABX-12-01, « Investissements d'avenir » program). The CBS belongs to the France-BioImaging infrastructure supported by the French National Research Agency (ANR-10-INBS-04, « Investments for the future »), the Labex EpiGenMed and is supported by the GIS "IBiSA: Infrastructures en Biologie Santé et Agronomie". AT and LO were supported by PhD fellowships from the Ministère de l'Education Nationale et de la Recherche. AT was supported by the Fondation Recherche Médicale (FRM FDT20140931071). AMC was supported by a PhD fellowship from Labex EpiGenMed and XR by the Beatriu de Pinos program of Agència de Gestió d'Ajuts Universitaris i de Recerca (AGAUR). AC was supported by ANR-13-BSV1-006 and PS by a PhD fellowship supported by the ANRT and CisBio.

AUTHOR CONTRIBUTION

AT, XR, AC, EM, PR, JPP and CG designed research; AT, XR, AC, AVE, FM, LO, PS, HB performed research; EM built the single molecule setup; AT, XR, AC, AVE, IS, FM, EM, FA, PR, JPP, CG analyzed data; AT, XR, AC, IS, EM, FA, JPP, CG wrote the paper.

CONFLICT OF INTEREST

The authors state no conflict of interest.

REFERENCES

- Acher, F. C., Bertrand, H. O., 2005. Amino acid recognition by Venus flytrap domains is encoded in an 8-residue motif. *Biopolymers* 80, 357-366.
- Acher, F. C., Selvam, C., Pin, J. P., Goudet, C., Bertrand, H. O., 2011. A critical pocket close to the glutamate binding site of mGlu receptors opens new possibilities for agonist design. *Neuropharmacology* 60, 102-107.
- Aronica, E., Gorter, J. A., Ijlst-Keizers, H., Rozemuller, A. J., Yankaya, B., Leenstra, S., Troost, D., 2003. Expression and functional role of mGluR3 and mGluR5 in human astrocytes and glioma cells: opposite regulation of glutamate transporter proteins. *Eur J Neurosci* 17, 2106-2118.
- Aronica, E., Gorter, J. A., Rozemuller, A. J., Yankaya, B., Troost, D., 2005. Activation of metabotropic glutamate receptor 3 enhances interleukin (IL)-1beta-stimulated release of IL-6 in cultured human astrocytes. *Neuroscience* 130, 927-933.
- Battaglia, G., Rizzoli, B., Bucci, D., Di Menna, L., Molinaro, G., Pallottino, S., Nicoletti, F., Bruno, V., 2015. Activation of mGlu3 metabotropic glutamate receptors enhances GDNF and GLT-1 formation in the spinal cord and rescues motor neurons in the SOD-1 mouse model of amyotrophic lateral sclerosis. *Neurobiol Dis* 74, 126-136.
- Ben-Ari, Y., Gaiarsa, J. L., Tyzio, R., Khazipov, R., 2007. GABA: a pioneer transmitter that excites immature neurons and generates primitive oscillations. *Physiol Rev* 87, 1215-1284.
- Cartmell, J., Adam, G., Chaboz, S., Henningsen, R., Kemp, J. A., Klingelschmidt, A., Metzler, V., Monsma, F., Schaffhauser, H., Wichmann, J., Mutel, V., 1998. Characterization of [³H]-*(2S,2'R,3'R)-2-(2',3'-dicarboxy-cyclopropyl)glycine* ([³H]-DCG IV) binding to metabotropic mGlu2 receptor-transfected cell membranes. *Br J Pharmacol* 123, 497-504.
- Celanire, S., Sebhat, I., Wichmann, J., Mayer, S., Schann, S., Gatti, S., 2015. Novel metabotropic glutamate receptor 2/3 antagonists and their therapeutic applications: a patent review (2005 - present). *Expert Opin Ther Pat* 25, 69-90.
- Consortium, S. W. G. o. t. P. G., 2014. Biological insights from 108 schizophrenia-associated genetic loci. *Nature* 511, 421-427.
- Corti, C., Battaglia, G., Molinaro, G., Rizzoli, B., Pittaluga, A., Corsi, M., Mugnaini, M., Nicoletti, F., Bruno, V., 2007. The use of knock-out mice unravels distinct roles for mGlu2 and mGlu3 metabotropic glutamate receptors in mechanisms of neurodegeneration/neuroprotection. *J Neurosci* 27, 8297-8308.
- De Filippis, B., Lyon, L., Taylor, A., Lane, T., Burnet, P. W., Harrison, P. J., Bannerman, D. M., 2015. The role of group II metabotropic glutamate receptors in cognition and anxiety:

- comparative studies in GRM2(-/-), GRM3(-/-) and GRM2/3(-/-) knockout mice. *Neuropharmacology* 89, 19-32.
- De Koninck, Y., 2007. Altered chloride homeostasis in neurological disorders: a new target. *Curr Opin Pharmacol* 7, 93-99.
- Di Menna, L., Joffe, M. E., Iacovelli, L., Orlando, R., Lindsley, C. W., Mairesse, J., Gressens, P., Cannella, M., Caraci, F., Copani, A., Bruno, V., Battaglia, G., Conn, P. J., Nicoletti, F., 2018. Functional partnership between mGlu3 and mGlu5 metabotropic glutamate receptors in the central nervous system. *Neuropharmacology* 128, 301-313.
- DiRaddo, J. O., Miller, E. J., Bowman-Dalley, C., Wroblewska, B., Javidnia, M., Grajkowska, E., Wolfe, B. B., Liotta, D. C., Wroblewski, J. T., 2015. Chloride is an Agonist of Group II and III Metabotropic Glutamate Receptors. *Mol Pharmacol* 88, 450-459.
- DiRaddo, J. O., Miller, E. J., Hathaway, H. A., Grajkowska, E., Wroblewska, B., Wolfe, B. B., Liotta, D. C., Wroblewski, J. T., 2014. A real-time method for measuring cAMP production modulated by Galphai/o-coupled metabotropic glutamate receptors. *J Pharmacol Exp Ther* 349, 373-382.
- Doornbos, M. L. J., Van der Linden, I., Vereyken, L., Tresadern, G., AP, I. J., Lavreysen, H., Heitman, L. H., 2018. Constitutive activity of the metabotropic glutamate receptor 2 explored with a whole-cell label-free biosensor. *Biochem Pharmacol* 152, 201-210.
- Doumazane, E., Scholler, P., Fabre, L., Zwier, J. M., Trinquet, E., Pin, J. P., Rondard, P., 2013. Illuminating the activation mechanisms and allosteric properties of metabotropic glutamate receptors. *Proc Natl Acad Sci U S A* 110, E1416-1425.
- Egan, M. F., Straub, R. E., Goldberg, T. E., Yakub, I., Callicott, J. H., Hariri, A. R., Mattay, V. S., Bertolino, A., Hyde, T. M., Shannon-Weickert, C., Akil, M., Crook, J., Vakkalanka, R. K., Balkissoon, R., Gibbs, R. A., Kleinman, J. E., Weinberger, D. R., 2004. Variation in GRM3 affects cognition, prefrontal glutamate, and risk for schizophrenia. *Proc Natl Acad Sci U S A* 101, 12604-12609.
- Engers, J. L., Rodriguez, A. L., Konkol, L. C., Morrison, R. D., Thompson, A. D., Byers, F. W., Blobaum, A. L., Chang, S., Venable, D. F., Loch, M. T., Niswender, C. M., Daniels, J. S., Jones, C. K., Conn, P. J., Lindsley, C. W., Emmitt, K. A., 2015. Discovery of a Selective and CNS Penetrant Negative Allosteric Modulator of Metabotropic Glutamate Receptor Subtype 3 with Antidepressant and Anxiolytic Activity in Rodents. *J Med Chem* 58, 7485-7500.
- Eriksen, L., Thomsen, C., 1995. [3H]-L-2-amino-4-phosphonobutyrate labels a metabotropic glutamate receptor, mGluR4a. *Br J Pharmacol* 116, 3279-3287.
- Fonnum, F., 1984. Glutamate: a neurotransmitter in mammalian brain. *J Neurochem* 42, 1-11.

- Frischknecht, R., Heine, M., Perraïs, D., Seidenbecher, C. I., Choquet, D., Gundelfinger, E. D., 2009. Brain extracellular matrix affects AMPA receptor lateral mobility and short-term synaptic plasticity. *Nat Neurosci* 12, 897-904.
- Goudet, C., Gaven, F., Kniazeff, J., Vol, C., Liu, J., Cohen-Gonsaud, M., Acher, F., Prezeau, L., Pin, J. P., 2004. Heptahelical domain of metabotropic glutamate receptor 5 behaves like rhodopsin-like receptors. *Proc Natl Acad Sci U S A* 101, 378-383.
- Goudet, C., Vilar, B., Courtiol, T., Deltheil, T., Bessiron, T., Brabet, I., Oueslati, N., Rigault, D., Bertrand, H. O., McLean, H., Daniel, H., Amalric, M., Acher, F., Pin, J. P., 2012. A novel selective metabotropic glutamate receptor 4 agonist reveals new possibilities for developing subtype selective ligands with therapeutic potential. *FASEB J* 26, 1682-1693.
- Harrison, P. J., Lyon, L., Sartorius, L. J., Burnet, P. W., Lane, T. A., 2008. The group II metabotropic glutamate receptor 3 (mGluR3, mGlu3, GRM3): expression, function and involvement in schizophrenia. *J Psychopharmacol* 22, 308-322.
- Jiang, C., Agulian, S., Haddad, G. G., 1992. Cl⁻ and Na⁺ homeostasis during anoxia in rat hypoglossal neurons: intracellular and extracellular in vitro studies. *J Physiol* 448, 697-708.
- Jiang, J. Y., Nagaraju, M., Meyer, R. C., Zhang, L., Hamelberg, D., Hall, R. A., Brown, E. M., Conn, P. J., Yang, J. J., 2014. Extracellular calcium modulates actions of orthosteric and allosteric ligands on metabotropic glutamate receptor 1alpha. *J Biol Chem* 289, 1649-1661.
- Johnson, B. G., Wright, R. A., Arnold, M. B., Wheeler, W. J., Ornstein, P. L., Schoepp, D. D., 1999. [3H]-LY341495 as a novel antagonist radioligand for group II metabotropic glutamate (mGlu) receptors: characterization of binding to membranes of mGlu receptor subtype expressing cells. *Neuropharmacology* 38, 1519-1529.
- Kaila, K., Price, T. J., Payne, J. A., Puskarjov, M., Voipio, J., 2014. Cation-chloride cotransporters in neuronal development, plasticity and disease. *Nat Rev Neurosci* 15, 637-654.
- Kalivas, P. W., 2009. The glutamate homeostasis hypothesis of addiction. *Nat Rev Neurosci* 10, 561-572.
- Kuang, D., Hampson, D. R., 2006. Ion dependence of ligand binding to metabotropic glutamate receptors. *Biochem Biophys Res Commun* 345, 1-6.
- Kubo, Y., Miyashita, T., Murata, Y., 1998. Structural basis for a Ca²⁺-sensing function of the metabotropic glutamate receptors. *Science* 279, 1722-1725.
- Kunz, M., 2014. Oncogenes in melanoma: an update. *Eur J Cell Biol* 93, 1-10.
- Laurie, D. J., Danzeisen, M., Boddeke, H. W., Sommer, B., 1995. Ligand binding profile of the rat metabotropic glutamate receptor mGluR3 expressed in a transfected cell line. *Naunyn Schmiedebergs Arch Pharmacol* 351, 565-568.

- Lewerenz, J., Maher, P., 2015. Chronic Glutamate Toxicity in Neurodegenerative Diseases-What is the Evidence? *Front Neurosci* 9, 469.
- Meldrum, B. S., 2000. Glutamate as a neurotransmitter in the brain: review of physiology and pathology. *J Nutr* 130, 1007S-1015S.
- Miladinovic, T., Nashed, M. G., Singh, G., 2015. Overview of Glutamatergic Dysregulation in Central Pathologies. *Biomolecules* 5, 3112-3141.
- Monn, J. A., Henry, S. S., Massey, S. M., Clawson, D. K., Chen, Q., Diseroad, B. A., Bhardwaj, R. M., Atwell, S., Lu, F., Wang, J., Russell, M., Heinz, B. A., Wang, X. S., Carter, J. H., Getman, B. G., Adragni, K., Broad, L. M., Sanger, H. E., Ursu, D., Catlow, J. T., Swanson, S., Johnson, B. G., Shaw, D. B., McKinzie, D. L., Hao, J., 2018. Synthesis and Pharmacological Characterization of C4beta-Amide-Substituted 2-Aminobicyclo[3.1.0]hexane-2,6-dicarboxylates. Identification of (1S,2S,4S,5S,6R)-2-Amino-4-[(3-methoxybenzoyl)amino]bicyclo[3.1.0]hexane-2,6-dicarboxylic Acid (LY2794193), a Highly Potent and Selective mGlu3 Receptor Agonist. *J Med Chem* 61, 2303-2328.
- Monn, J. A., Prieto, L., Taboada, L., Hao, J., Reinhard, M. R., Henry, S. S., Beadle, C. D., Walton, L., Man, T., Rudyk, H., Clark, B., Tupper, D., Baker, S. R., Lamas, C., Montero, C., Marcos, A., Blanco, J., Bures, M., Clawson, D. K., Atwell, S., Lu, F., Wang, J., Russell, M., Heinz, B. A., Wang, X., Carter, J. H., Getman, B. G., Catlow, J. T., Swanson, S., Johnson, B. G., Shaw, D. B., McKinzie, D. L., 2015a. Synthesis and Pharmacological Characterization of C4-(Thiotriazolyl)-substituted-2-aminobicyclo[3.1.0]hexane-2,6-dicarboxylates. Identification of (1R,2S,4R,5R,6R)-2-Amino-4-(1H-1,2,4-triazol-3-ylsulfanyl)bicyclo[3.1.0]hexane-2,6-dicarboxylic Acid (LY2812223), a Highly Potent, Functionally Selective mGlu2 Receptor Agonist. *J Med Chem* 58, 7526-7548.
- Monn, J. A., Prieto, L., Taboada, L., Pedregal, C., Hao, J., Reinhard, M. R., Henry, S. S., Goldsmith, P. J., Beadle, C. D., Walton, L., Man, T., Rudyk, H., Clark, B., Tupper, D., Baker, S. R., Lamas, C., Montero, C., Marcos, A., Blanco, J., Bures, M., Clawson, D. K., Atwell, S., Lu, F., Wang, J., Russell, M., Heinz, B. A., Wang, X., Carter, J. H., Xiang, C., Catlow, J. T., Swanson, S., Sanger, H., Broad, L. M., Johnson, M. P., Knopp, K. L., Simmons, R. M., Johnson, B. G., Shaw, D. B., McKinzie, D. L., 2015b. Synthesis and pharmacological characterization of C4-disubstituted analogs of 1S,2S,5R,6S-2-aminobicyclo[3.1.0]hexane-2,6-dicarboxylate: identification of a potent, selective metabotropic glutamate receptor agonist and determination of agonist-bound human mGlu2 and mGlu3 amino terminal domain structures. *J Med Chem* 58, 1776-1794.

- Mudo, G., Trovato-Salinaro, A., Caniglia, G., Cheng, Q., Condorelli, D. F., 2007. Cellular localization of mGluR3 and mGluR5 mRNAs in normal and injured rat brain. *Brain Res* 1149, 1-13.
- Mutel, V., Ellis, G. J., Adam, G., Chaboz, S., Nilly, A., Messer, J., Bleuel, Z., Metzler, V., Malherbe, P., Schlaeger, E. J., Roughley, B. S., Faull, R. L., Richards, J. G., 2000. Characterization of [³H]Quisqualate binding to recombinant rat metabotropic glutamate 1a and 5a receptors and to rat and human brain sections. *J Neurochem* 75, 2590-2601.
- Nicoletti, F., Bockaert, J., Collingridge, G. L., Conn, P. J., Ferraguti, F., Schoepp, D. D., Wroblewski, J. T., Pin, J. P., 2011. Metabotropic glutamate receptors: from the workbench to the bedside. *Neuropharmacology* 60, 1017-1041.
- Nicoletti, F., Bruno, V., Ngomba, R. T., Gradini, R., Battaglia, G., 2015. Metabotropic glutamate receptors as drug targets: what's new? *Curr Opin Pharmacol* 20, 89-94.
- O'Brien, N. L., Way, M. J., Kandaswamy, R., Fiorentino, A., Sharp, S. I., Quadri, G., Alex, J., Anjorin, A., Ball, D., Cherian, R., Dar, K., Gormez, A., Guerrini, I., Heydtmann, M., Hillman, A., Lankappa, S., Lydall, G., O'Kane, A., Patel, S., Quested, D., Smith, I., Thomson, A. D., Bass, N. J., Morgan, M. Y., Curtis, D., McQuillin, A., 2014. The functional GRM3 Kozak sequence variant rs148754219 affects the risk of schizophrenia and alcohol dependence as well as bipolar disorder. *Psychiatr Genet* 24, 277-278.
- Ohishi, H., Shigemoto, R., Nakanishi, S., Mizuno, N., 1993. Distribution of the mRNA for a metabotropic glutamate receptor (mGluR3) in the rat brain: an in situ hybridization study. *J Comp Neurol* 335, 252-266.
- Olofsson, L., Felekyan, S., Doumazane, E., Scholler, P., Fabre, L., Zwier, J. M., Rondard, P., Seidel, C. A., Pin, J. P., Margeat, E., 2014. Fine tuning of sub-millisecond conformational dynamics controls metabotropic glutamate receptors agonist efficacy. *Nat Commun* 5, 5206.
- Olofsson, L., Margeat, E., 2013. Pulsed interleaved excitation fluorescence spectroscopy with a supercontinuum source. *Opt Express* 21, 3370-3378.
- Pin, J. P., Bettler, B., 2016. Organization and functions of mGlu and GABAB receptor complexes. *Nature* 540, 60-68.
- Rozas, I., Alkorta, I., Elguero, J., 2008. Hydrogen bonds and Coulombic interactions: a theoretical study. *Struct. Chem* 19, 923-933.
- Scholler, P., Moreno-Delgado, D., Lecat-Guillem, N., Doumazane, E., Monnier, C., Charrier-Savournin, F., Fabre, L., Chouvet, C., Soldevila, S., Lamarque, L., Donsimoni, G., Roux, T., Zwier, J. M., Trinquet, E., Rondard, P., Pin, J. P., 2017. HTS-compatible FRET-based conformational sensors clarify membrane receptor activation. *Nat Chem Biol.*

- Schweitzer, C., Kratzeisen, C., Adam, G., Lundstrom, K., Malherbe, P., Ohresser, S., Stadler, H., Wichmann, J., Woltering, T., Mutel, V., 2000. Characterization of [(3)H]-LY354740 binding to rat mGlu2 and mGlu3 receptors expressed in CHO cells using semliki forest virus vectors. *Neuropharmacology* 39, 1700-1706.
- Selvam, C., Lemasson, I. A., Brabet, I., Oueslati, N., Karaman, B., Cabaye, A., Tora, A. S., Commare, B., Courtiol, T., Cesarini, S., McCort-Tranchepain, I., Rigault, D., Mony, L., Bessiron, T., McLean, H., Leroux, F. R., Colobert, F., Daniel, H., Goupil-Lamy, A., Bertrand, H. O., Goudet, C., Pin, J. P., Acher, F. C., 2018. Increased Potency and Selectivity for Group III Metabotropic Glutamate Receptor Agonists Binding at Dual sites. *J Med Chem* 61, 1969-1989.
- Staley, K. J., Soldo, B. L., Proctor, W. R., 1995. Ionic mechanisms of neuronal excitation by inhibitory GABAA receptors. *Science* 269, 977-981.
- Sykova, E., Nicholson, C., 2008. Diffusion in brain extracellular space. *Physiol Rev* 88, 1277-1340.
- Tamaru, Y., Nomura, S., Mizuno, N., Shigemoto, R., 2001. Distribution of metabotropic glutamate receptor mGluR3 in the mouse CNS: differential location relative to pre- and postsynaptic sites. *Neuroscience* 106, 481-503.
- Thompson, J. D., Higgins, D. G., Gibson, T. J., 1994. CLUSTAL W: improving the sensitivity of progressive multiple sequence alignment through sequence weighting, position-specific gap penalties and weight matrix choice. *Nucleic Acids Res* 22, 4673-4680.
- Thomsen, C., Mulvihill, E. R., Haldeman, B., Pickering, D. S., Hampson, D. R., Suzdak, P. D., 1993. A pharmacological characterization of the mGluR1 alpha subtype of the metabotropic glutamate receptor expressed in a cloned baby hamster kidney cell line. *Brain Res* 619, 22-28.
- Tora, A. S., Rovira, X., Dione, I., Bertrand, H. O., Brabet, I., De Koninck, Y., Doyon, N., Pin, J. P., Acher, F., Goudet, C., 2015. Allosteric modulation of metabotropic glutamate receptors by chloride ions. *FASEB J* 29, 4174-4188.
- Tremblay, M. E., Lowery, R. L., Majewska, A. K., 2010. Microglial interactions with synapses are modulated by visual experience. *PLoS Biol* 8, e1000527.
- Trinquet, E., Fink, M., Bazin, H., Grillet, F., Maurin, F., Bourrier, E., Ansanay, H., Leroy, C., Michaud, A., Durroux, T., Maurel, D., Malhaire, F., Goudet, C., Pin, J. P., Naval, M., Hernout, O., Chretien, F., Chapleur, Y., Mathis, G., 2006. D-myo-inositol 1-phosphate as a surrogate of D-myo-inositol 1,4,5-tris phosphate to monitor G protein-coupled receptor activation. *Anal Biochem* 358, 126-135.
- Vafabakhsh, R., Levitz, J., Isacoff, E. Y., 2015. Conformational dynamics of a class C G-protein-coupled receptor. *Nature* 524, 497-501.

- Van Hemelrijck, A., Sarre, S., Smolders, I., Michotte, Y., 2005. Determination of amino acids associated with cerebral ischaemia in rat brain microdialysates using narrowbore liquid chromatography and fluorescence detection. *J Neurosci Methods* 144, 63-71.
- Vardi, N., Duvoisin, R., Wu, G., Sterling, P., 2000. Localization of mGluR6 to dendrites of ON bipolar cells in primate retina. *J Comp Neurol* 423, 402-412.
- Wang, W., Kiyoshi, C. M., Du, Y., Ma, B., Alford, C. C., Chen, H., Zhou, M., 2016. mGluR3 Activation Recruits Cytoplasmic TWIK-1 Channels to Membrane that Enhances Ammonium Uptake in Hippocampal Astrocytes. *Mol Neurobiol* 53, 6169-6182.
- Widengren, J., Kudryavtsev, V., Antonik, M., Berger, S., Gerken, M., Seidel, C. A., 2006. Single-molecule detection and identification of multiple species by multiparameter fluorescence detection. *Anal Chem* 78, 2039-2050.
- Wright, R. A., Arnold, M. B., Wheeler, W. J., Ornstein, P. L., Schoepp, D. D., 2000. Binding of [³H](2S,1'S,2'S)-2-(9-xanthylmethyl)-2-(2'-carboxycyclopropyl) glycine ([³H]LY341495) to cell membranes expressing recombinant human group III metabotropic glutamate receptor subtypes. *Naunyn Schmiedebergs Arch Pharmacol* 362, 546-554.
- Yi, H., Geng, L., Black, A., Talmon, G., Berim, L., Wang, J., 2017. The miR-487b-3p/GRM3/TGFbeta signaling axis is an important regulator of colon cancer tumorigenesis. *Oncogene*.
- Zhang, C., Huang, Y., Jiang, Y., Mulpuri, N., Wei, L., Hamelberg, D., Brown, E. M., Yang, J. J., 2014. Identification of an L-phenylalanine binding site enhancing the cooperative responses of the calcium-sensing receptor to calcium. *J Biol Chem* 289, 5296-5309.

FIGURES

Figure 1: The Venus flytrap domain is required for mGlu₃ receptor high basal activity.

(A) Signaling activity of the eight mGluRs quantified by inositol monophosphate (IP1) production under vehicle (VEH) or 1 mM glutamate (Glu) stimulation. HTRF ratio is inversely proportional to IP1 levels. Among all mGluRs, mGlu₃ receptor low HTRF ratio in vehicle condition suggests a high basal activity. Each data point corresponds to means ± SEM of at 6 experiments. (B-C) Glutamate concentration-response curves of mGlu₂ and mGlu₃ receptors chimeras determined by IP1 (B) and TR-FRET mGlu sensor (C) assays. Contrary to mGlu₂ receptor (full circles), mGlu₃ receptor (full squares) concentration-response curve is nearly flat due to its high basal activity. This is abolished when mGlu₃ VFT is replaced by the one from mGlu₂ receptor (VFT2/TMD3, open squares). In contrast, fusion of mGlu₃ VFT to mGlu₂ TMD (VFT3/TMD2 chimera, open circles) results to an mGlu₃ receptor-like concentration response curve, indicating mGlu₃ VFT supports the receptor's high basal activity. Each data point corresponds to means ± SEM of at 3 experiments. (D) Principle of TR-FRET mGlu sensors. Concentration-response curve parameters are listed in supplemental table 1. *** p<0.001 according to One-way ANOVA with Dunnett's post test. CRD: Cysteine-rich domain; ECD: Extracellular domain; Glu: Glutamate; TMD: Transmembrane domain; VEH: vehicle; VFT: Venus flytrap.

Figure 2: Glutamate binding is required for mGlu₃ receptor high basal activity.

(A) TR-FRET ratios measured in mGlu3 expressing cells in absence (VEH) and presence of 1mM glutamate (Glu) or the competitive antagonist LY341495. Basal activity of mGlu₃ receptors is decreased by LY341495 addition. Each data point corresponds to means ± SEM of at 11 experiments. (B) Glutamate concentration-response curves of mGlu3 T174A (lozenges) and WT receptors (circles) determined by TR-FRET mGlu sensor assay. The glutamate-insensitive mutant T174A did not show low FRET ratios in the vehicle condition (VEH) as compared to the WT, indicating basal activity of the receptor is linked to glutamate. Each data point corresponds to mean ± SEM of at 3 experiments. Data are normalized by VEH FRET window

(A) or top and bottom the WT concentration-response curve **(B)**. ECD: Extracellular domain; Glu: Glutamate; TMD: Transmembrane domain; VEH: vehicle.

Figure 3: Extracellular chloride ions enhance mGlu₃ receptor activation by glutamate.

(A) Glutamate concentration-response curves determined on mGlu₃ receptors by measuring TR-FRET ratios in a buffer containing a standard Cl⁻ concentration (high Cl⁻, full circles) and in a Cl⁻ - depleted buffer (low Cl⁻, open circles). Data indicate that Cl⁻ both potentiate basal activity of the receptor (VEH condition) and glutamate potency. The latter can be re-calculated by extrapolation in the high Cl⁻ buffer, by subtracting the basal activity (red curve). Each data point corresponds to means ± SEM of 11 experiments. Extrapolated glutamate potency value is listed in supplemental table 2, and matches glutamate Ki determined in supplemental figure 2. **(B)** TR-FRET experiments in increasing Cl⁻ concentrations indicate both mGlu₃ basal activity and glutamate potency are potentiated by Cl⁻ in a concentration-dependent manner. Each data point corresponds to means ± SEM of 5 experiments. **(C)** Cl⁻ concentration-response curves in absence (VEH, open squares) and presence of 30 μM glutamate (EC₈₀, full squares). Each data point corresponds to means ± SEM of 5 experiments. Cl⁻ potency was estimated to 30.98 mM with glutamate. In vehicle condition, Cl⁻ potency was extrapolated to 470.10 mM. **(D)** Glutamate concentration-response curve on mGlu₂ receptors determined by TR-FRET mGlu sensor assay. Each data point corresponds to means ± SEM of 3 experiments. **(E)** TR-FRET levels on mGlu₃ receptors in absence of ligand (VEH) and in presence of 1 mM LY341495 (LY34, competitive antagonist) or glutamate (Glu) in high and low Cl⁻ buffers. mGlu₃ basal response (VEH) in high Cl⁻ is abolished by LY341495 to a similar FRET level observed in low Cl⁻. Each data point corresponds to mean ± SEM of 11 experiments. Data are normalized by largest signal window defined by top and bottom of the curve in low Cl⁻. Concentration-response curve parameters are listed in supplemental table 2. Glu: glutamate; LY34: LY341495; VEH: vehicle.

Figure 4: Chloride ions strongly favor glutamate-induced active conformation of mGlu₃ receptors.

(A) TR-FRET ratios of mGlu₃ WT and T174A receptors measured in absence (VEH) and presence of 30 μM (EC₈₀) glutamate. Each data point corresponds to means ± SEM of 11 (mGlu₃ WT) and 3 experiments (mGlu₃ T174A). **(B)** Principle of smFRET applied to mGluRs. **(C)** Apparent FRET efficiency (E_{PR}) of mGlu₃ WT and T174A purified ECDs in absence (VEH) and presence of 1 mM glutamate, measured in smFRET. These results correlate data in **(A)** and suggest that basal activity of mGlu₃ receptor is due to Cl⁻ potentiation of

glutamate-induced active conformation and not to an agonist activity of Cl⁻. Each data point corresponds to means ± SEM of 3 (mGlu₃ WT) and 4 experiments (mGlu₃ T174A). E_{PR} values are shown in supplemental figure 4. *** p<0.001 according One-way ANOVA with Sidak's post test. ECD: extracellular domain; Glu, glutamate (for TR-FRET experiments, EC₈₀ i.e. 30μM as determined in WT high Cl⁻ concentration-response curve; for smFRET, 1 mM); GPI: Glycosylphosphatidyl inositol; LY34, LY341495; n.s.: non significant; PLC: Phospholipase C; TMD: transmembrane domain; VEH, vehicle.

Figure 5: Different molecular and structural determinants of glutamate and chloride binding in mGlu₂ and mGlu₃ receptors

(A-B) mGlu₂ and mGlu₃ Acc VFT 3D-structures (PDB 4XAQ and 5CNK). Monomers (blue trace) are displayed in panel A, front view of dimers (blue and green traces) in panel B. Halides at site 1 and 2 as defined in Tora et al 2015, are displayed with van der Waals spheres. In mGlu₂ receptor, α-helix 7 holds 4 turns (colored in red and orange for the first turn) and loop 7 (between β-strand 7 and α-helix 7) adopts a straight conformation (orange). In mGlu₃ receptor, α-helix 7 is made of only 3 turns (colored in red) as turn 1 is unfolded allowing loop 7 (in orange) to curl. Ca distances are displayed between green chain (Glu222 for mGlu₂ receptor, Glu228 for mGlu₃ receptor) and blue chain (Ser 246 and Val 253 for mGlu₂ receptor, Ile252 and Val259 for mGlu₃ receptor). The hairpin structure preceding α-helix 1 (I47 to N61) is named loop 1 and colored in purple. (C) mGlu₂ receptor (left panel): R243 (loop 7 in lobe 2) is tightly bound to D95 (loop 2 between β-strand 2 and α-helix 2) and D146 (loop 3 between β-strand 3 and α-helix 3) in lobe 1 by two salt bridges, mGlu3 receptor (right panel) R249 is not binding to D102 (loop 2), the homologous residues to mGlu2 D95 but to the carbonyl of G51 of loop 1 which is possible because of the twisted loop 7 in the active dimer. This distortion allows several inter-dimer interactions: I252 with A176, R253 and K 246 with E228. (D). The closed mGlu2 VFT is further stabilized by an ionic interaction between D146 (loop 3) and R271 (loop 8 between β-strand 8 and α-helix 8) and a cation-Π interaction between Y144 (loop 3) and R271 in mGlu₂ receptor (left panel). In mGlu₃ receptor, a similar cation-Π interaction between Y150 and R277 is present in the Resting closed closed dimer conformation, Rcc (PDB structure 2E4U) and in the Acc conformation (central and right panel). However, the distance is too long between S152 and R277 for a direct interaction. It is

mediated by a water molecule (red atom, central panel) in the RCC conformation or by a halide (iodide in 5CNK, violet atom, right panel) ion in the superstable ACC conformation (Supplemental Figure 7). Atom color code: C chain color, N blue, O red, Cl green, I violet. (E) Mutations of S152 in mGlu3 into an alanine (S152A, squares) or aspartate (S152D, triangles) both reduce receptor basal activity without significantly reducing glutamate potency in TR-FRET sensor assay. Each data point corresponds to mean \pm SEM of 6 to 11 experiments (see details in supplemental figure 2). Concentration-response curve parameters are listed in supplemental table S2. Glu: glutamate; VEH: vehicle.

Figure 6. A unique “chloride lock” stabilizes the glutamate-induced active state of the mGlu₃ receptor.

(A-B) 3D-structures displaying the key residues involved in the stabilization of the closed state of the VFT of mGlu₂ and mGlu₃ receptors (PDB 4XAQ and 5CNK). Interactions are displayed as dashed lines. (C-D). Schematic representation of the interaction network in the cleft between the two lobes of the VFT of mGlu₂ and mGlu₃ receptors. Color code see Figure 5.

Figure 1

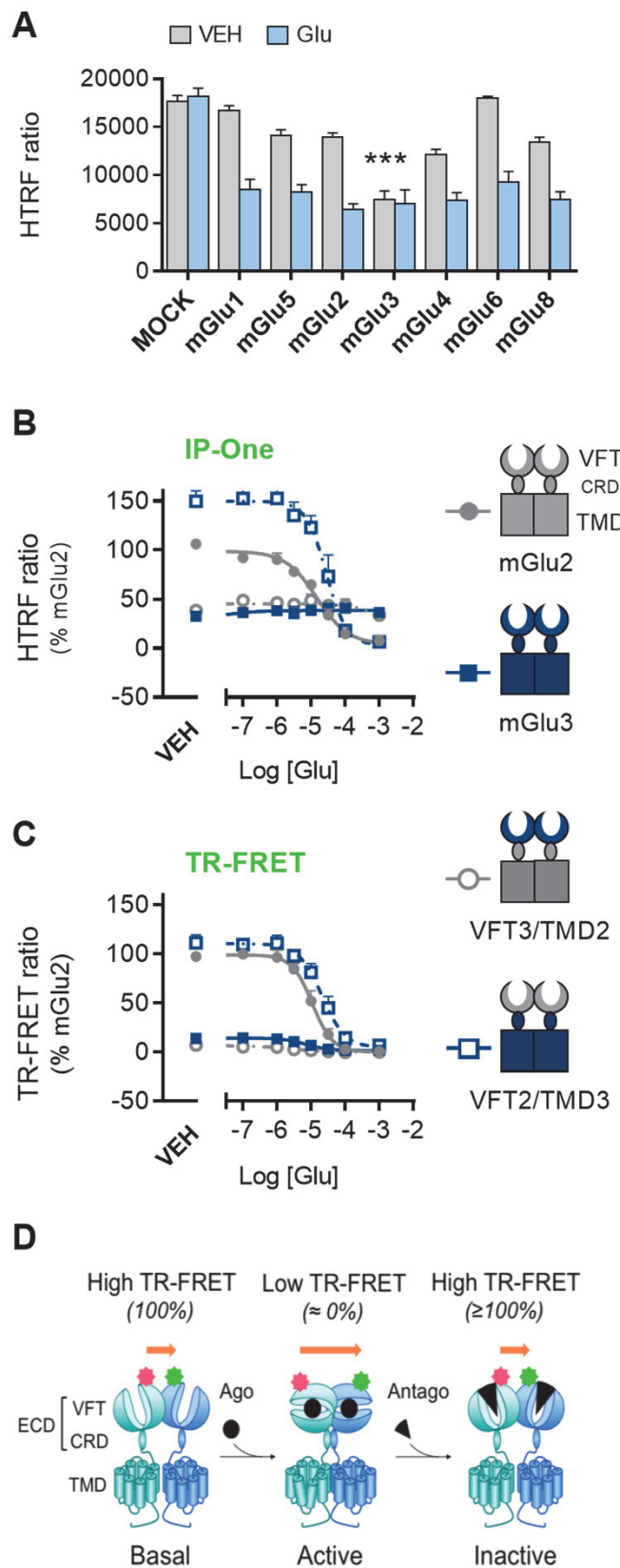
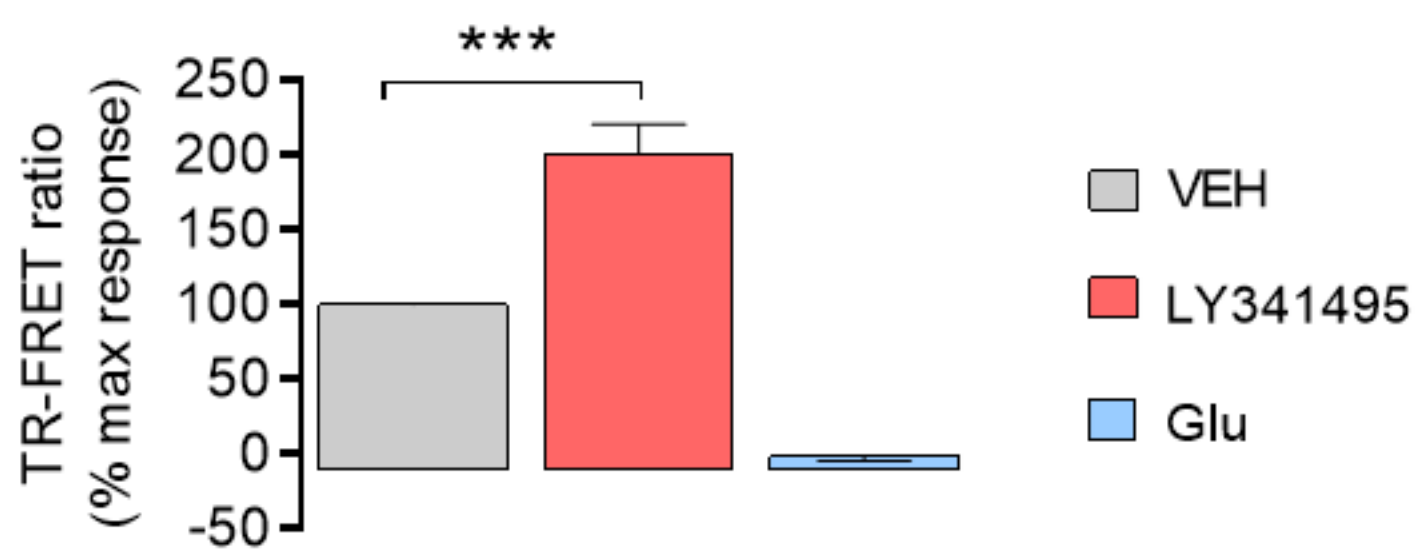


Figure 2

A



B

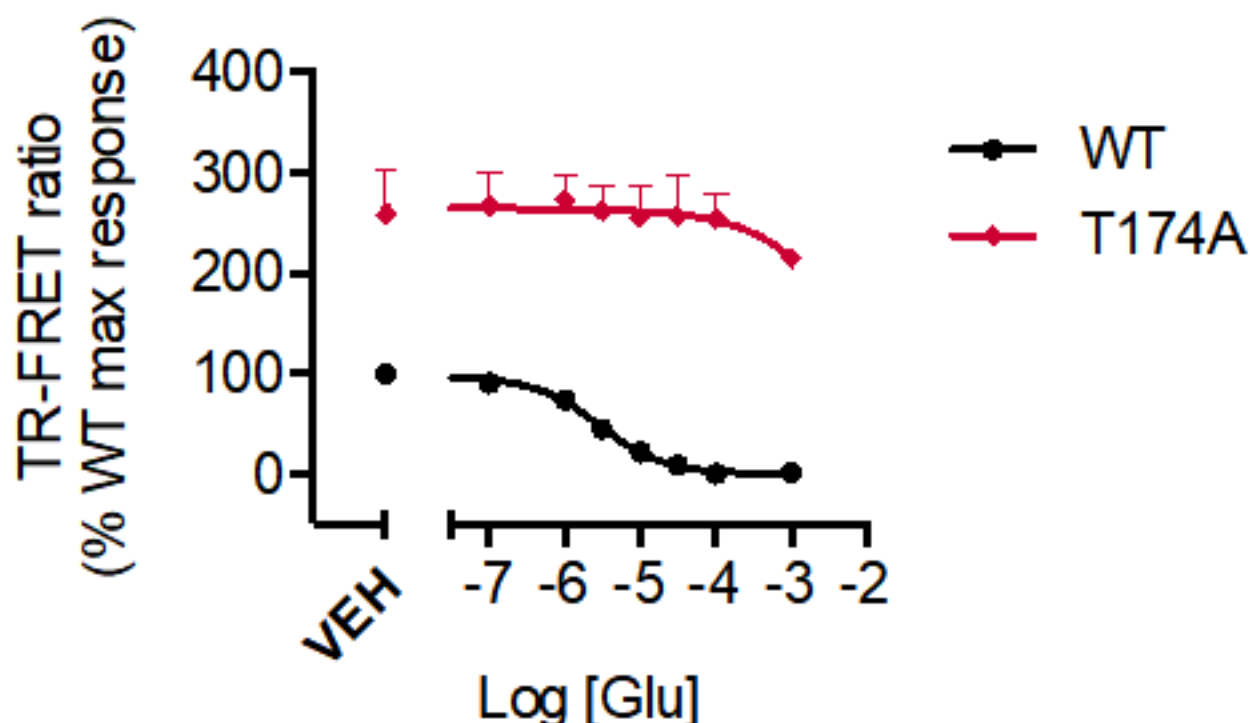
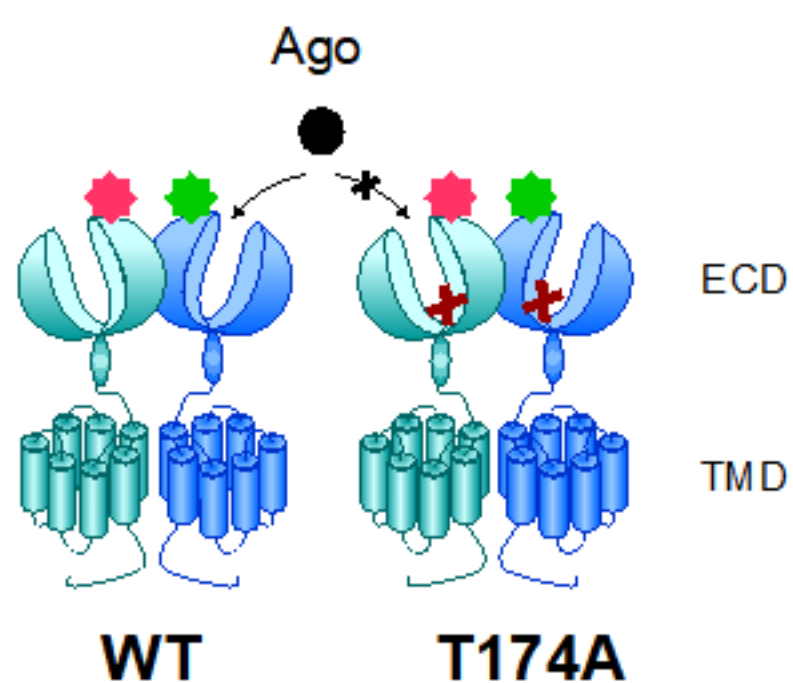


Figure 3

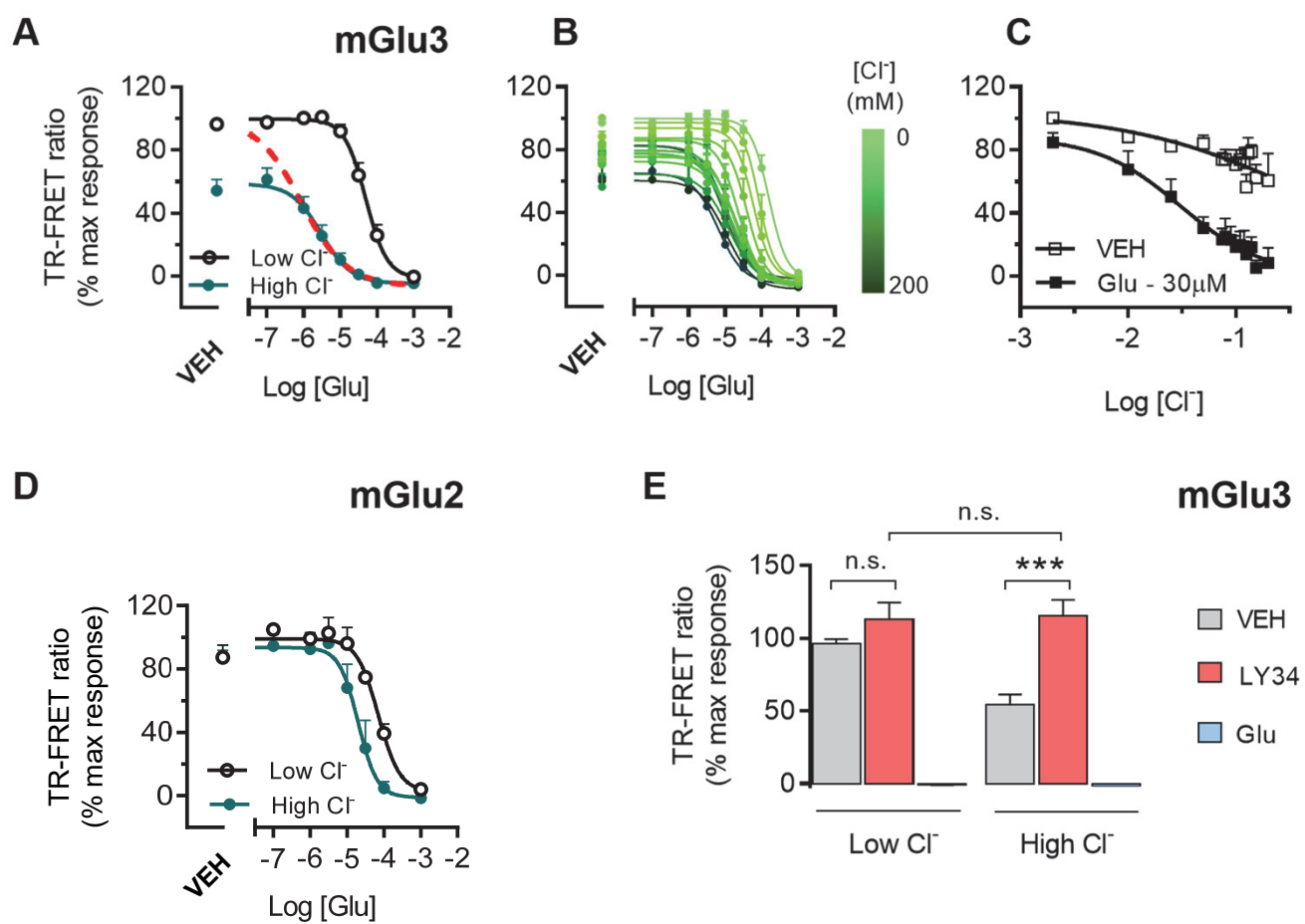


Figure 4

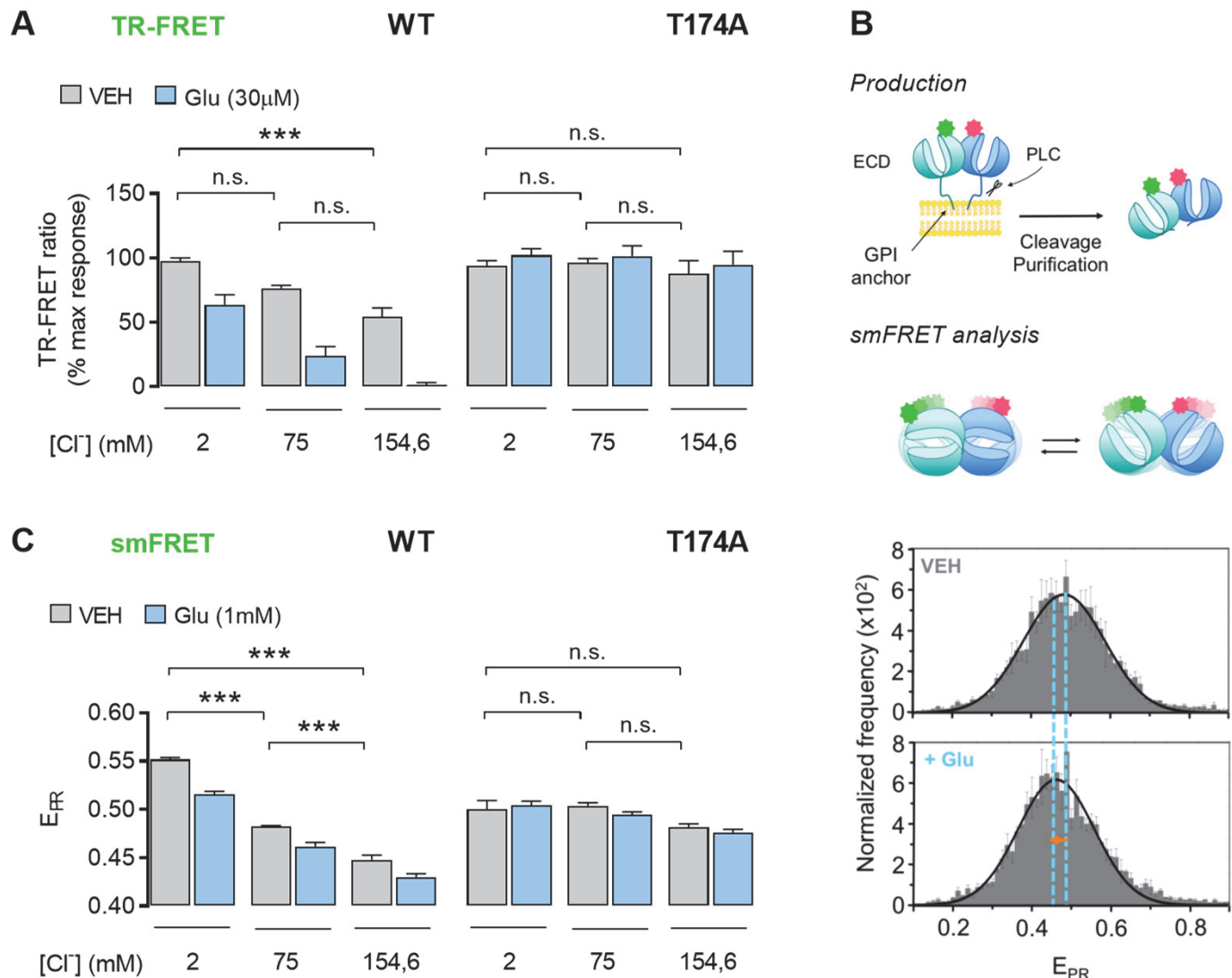


Figure 5

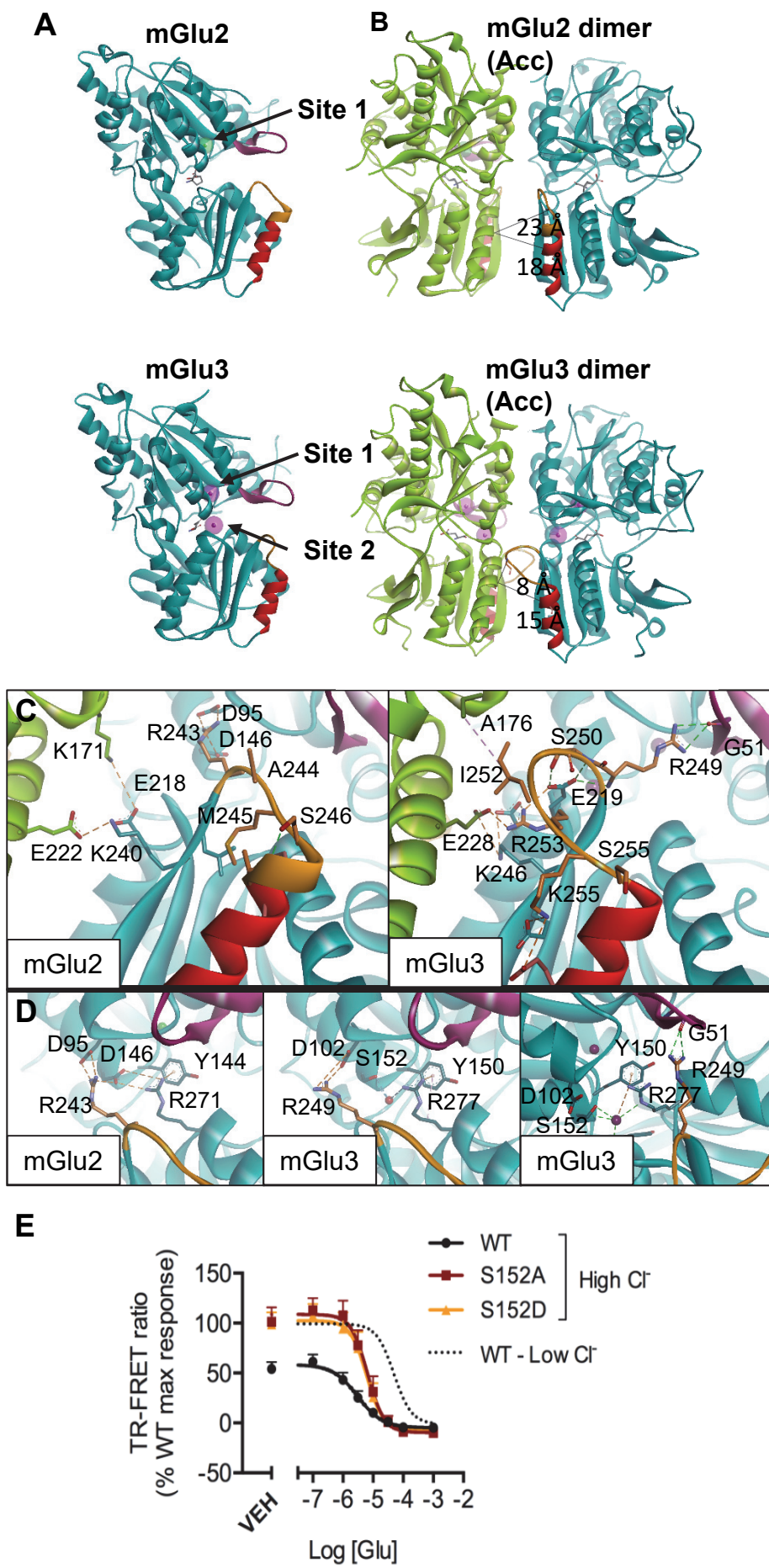


Figure 6

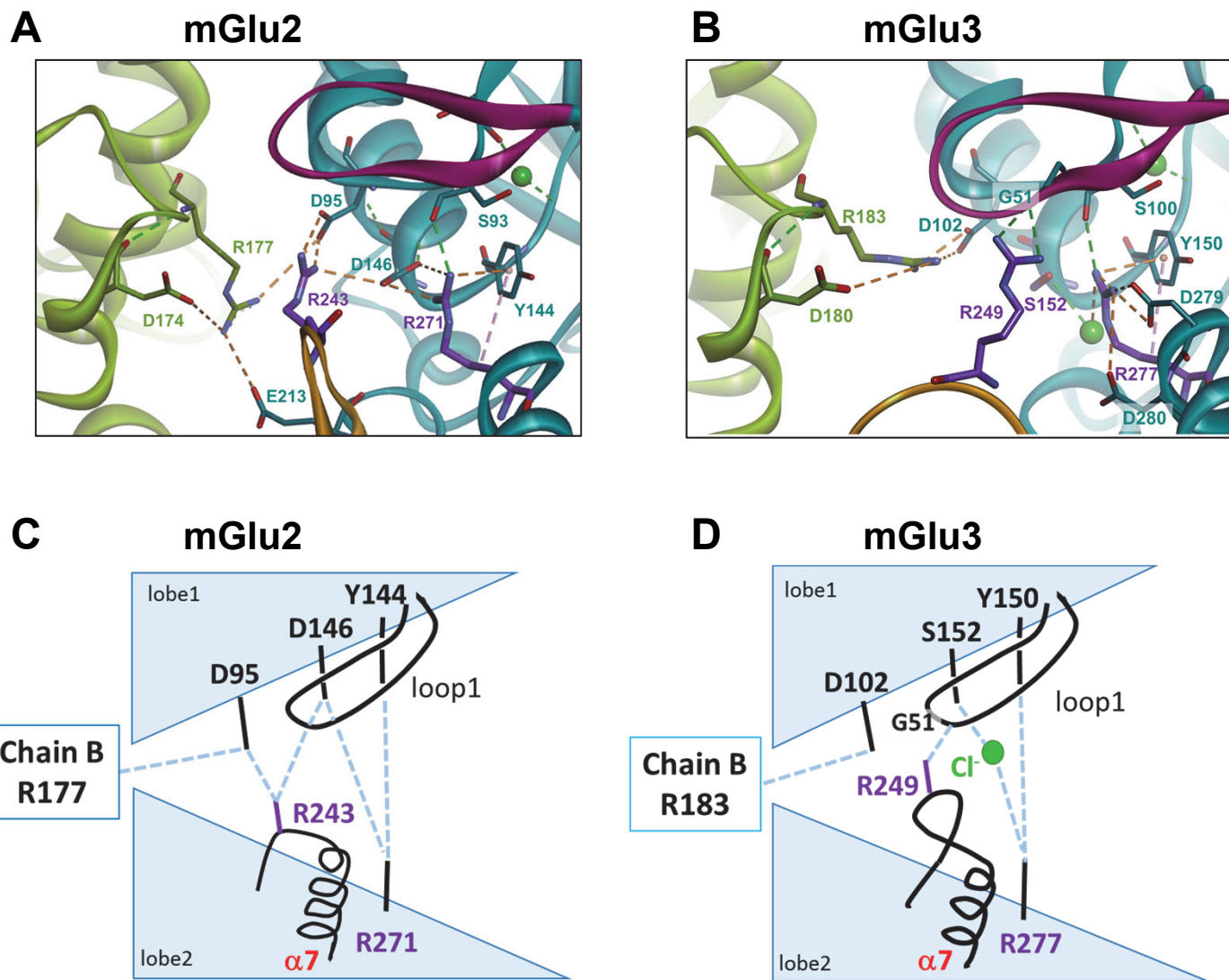


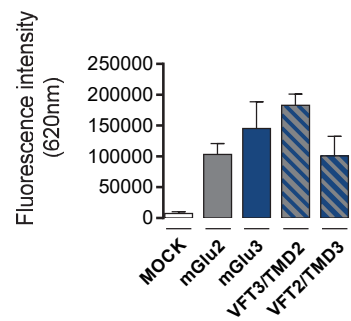
Table 1

	[Glutamate] (μ M)
Plated cells post-transfection (t=0)	
1x wash with sensor buffer - EAAC1	1,33 ± 0,12
1x wash with sensor buffer + EAAC1	1,39 ± 0,23
Plated cells before experiments (t=2h)	
in glutamax™ - EAAC1	3,27 ± 0,004
in glutamax™ + EAAC1	0,59 ± 0,03
Plated cells before experiments (t=5h)	
in glutamax™ - EAAC1	> 5
in glutamax™ + EAAC1	1,36 ± 0,01
Extracellular medium	
Glutamax™	0,07 ± 0,01
IP-One buffer	0,43 ± 0,03
Ca ²⁺ /Sensor buffer	≈ 0

Table 1: Extracellular media residual glutamate concentrations.

Glutamate concentrations found in different media used in our transient expression system. Data were determined on supernatant from freshly washed plated cells after 24h transfection (t=0), 2 or 5h after medium change by Glutamax™ (before experiments, see material and methods section for details) and on various buffers. Effect of glutamate transporter EAAC1 co-expression was also assessed. Values represent mean ± S.E.M of n=3 experiments. Sensor and Ca²⁺ buffers correspond to high Cl⁻ buffer composition.

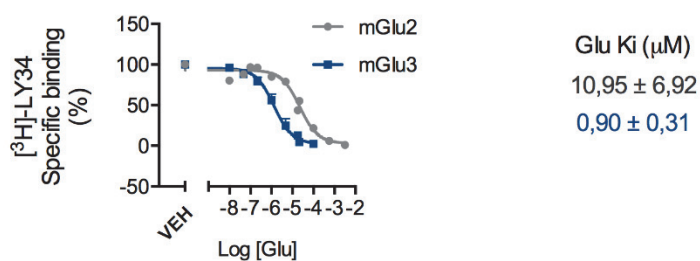
Supplemental Figure 1



Supplemental figure 1: Expression levels of mGlu2 and mGlu3 chimeras.

Quantification by fluorescence at 620nm on Lumi4-Tb labeled receptors transiently expressed in HEK293 cells.

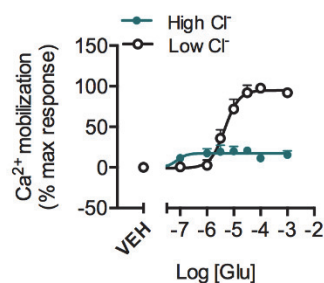
Supplemental figure 2



Supplemental figure 2: Glutamate affinity of mGlu2 and mGlu3 receptors.

Displacement of [³H]-LY341495 by increasing concentrations of glutamate (Glu) on mGlu2 and mGlu3 receptors. Values obtained from vehicle (VEH) condition were used to define 100% of the signal. mGlu2 and mGlu3 expressing membranes were incubated with 5nM and 3nM of [³H]-LY341495 respectively (corresponding to ≈ K_d of this radioligand)

Supplemental figure 3

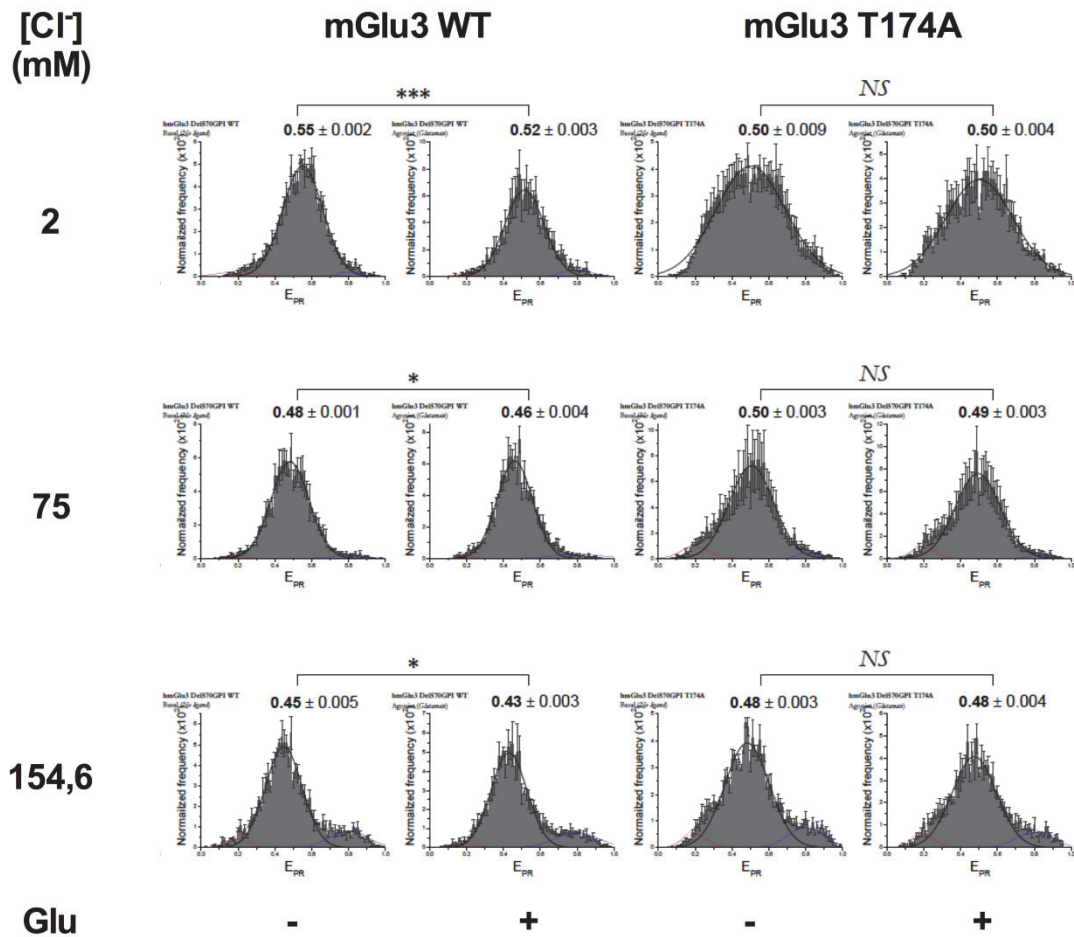


Supplemental figure 3: Chloride sensitivity of mGlu3 receptor.

Glutamate concentration-response curves derived from Ca²⁺ mobilization data obtained in high (full circles) and low Cl⁻ (open circles) buffers.

Data are normalized by the largest signal window defined by the top and bottom of the curve in low Cl⁻. Curve parameters are listed in supplemental table 2. Glu: glutamate; VEH: vehicle

Supplemental figure 4



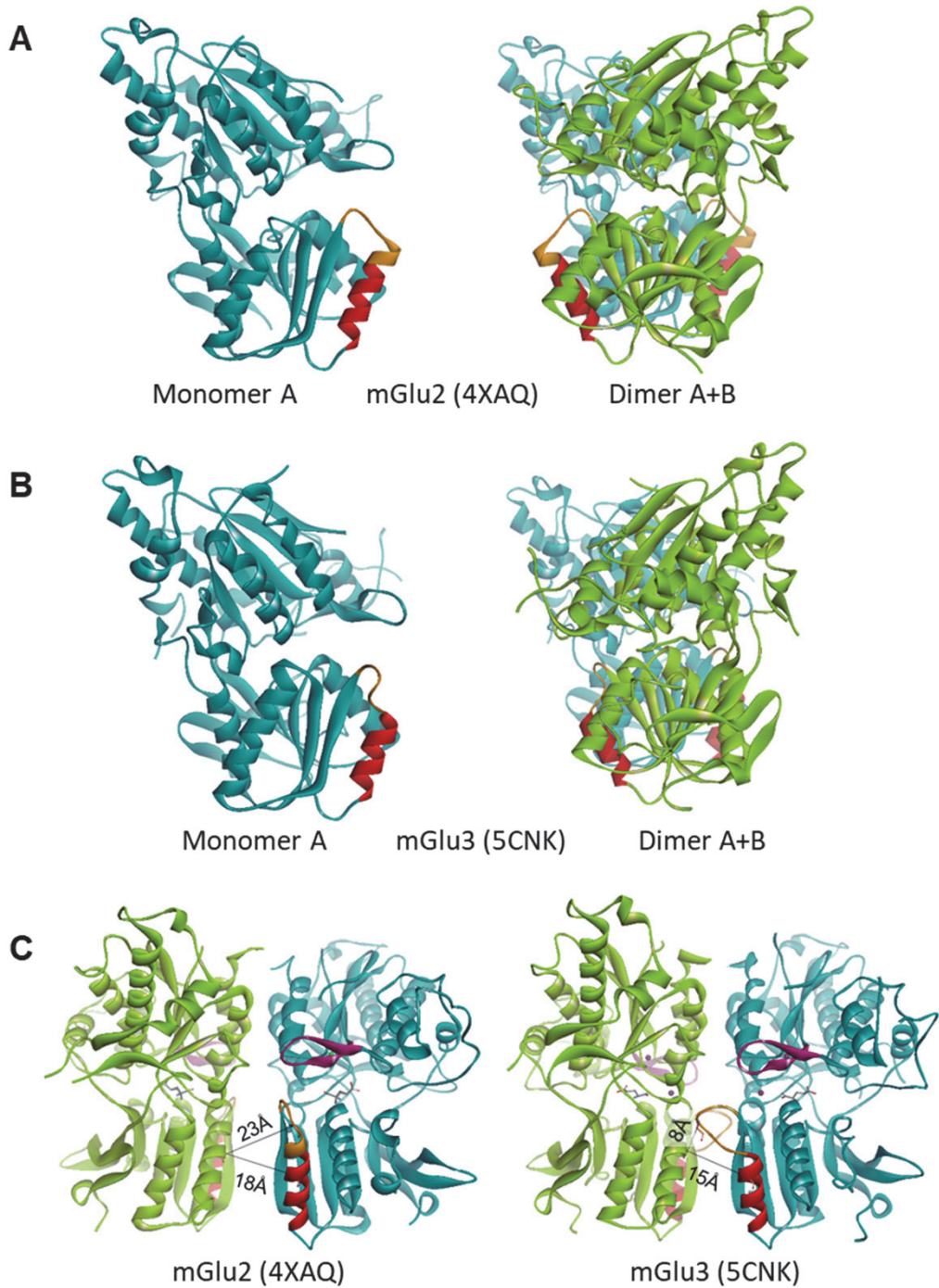
Supplemental figure 4: smFRET data of mGlu3 WT and T174A receptors.

Apparent FRET efficiencies (E_{PR}) were measured on purified mGlu3 WT and T174A extracellular domains in absence (vehicle, -) and 1mM glutamate stimulation (+) in 2, 75 and 154,6mM Cl⁻ buffers.

*** p<0,001, *p<0,05 according t-test.

N.S.: non significant.

Supplemental figure 5

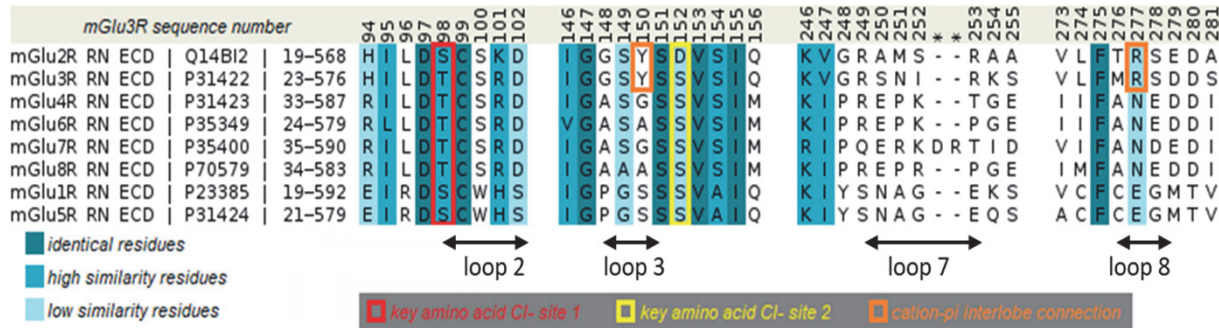


Supplemental figure 5: 3D Structures of VFT mGlu₂ and mGlu₃ receptor dimers in their active conformation (Acc).

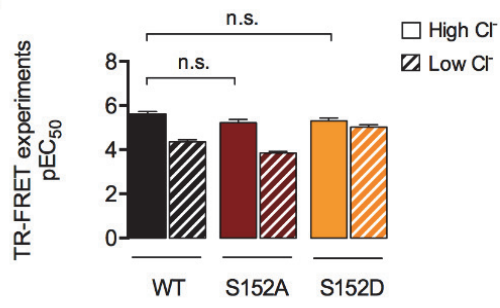
(A-B) side view. (C) front view same figure as Fig.5. Color code see Fig.5. Comparison of dimers in A and B, reveals a larger dimer contact surface in mGlu3 Acc which may be considered as a superstable dimer conformation.

Supplemental figure 6

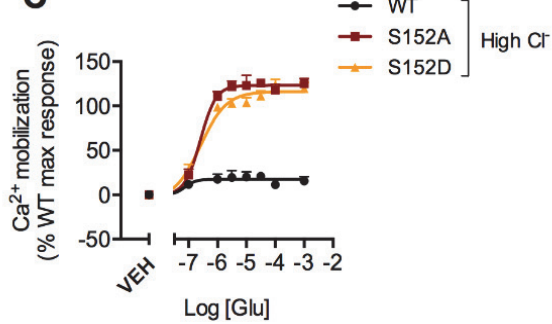
A



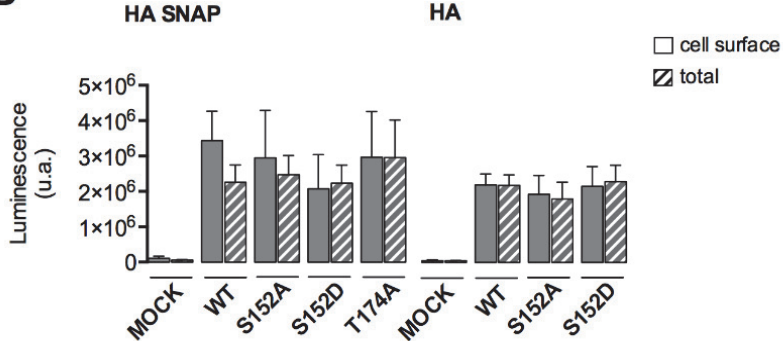
B



C



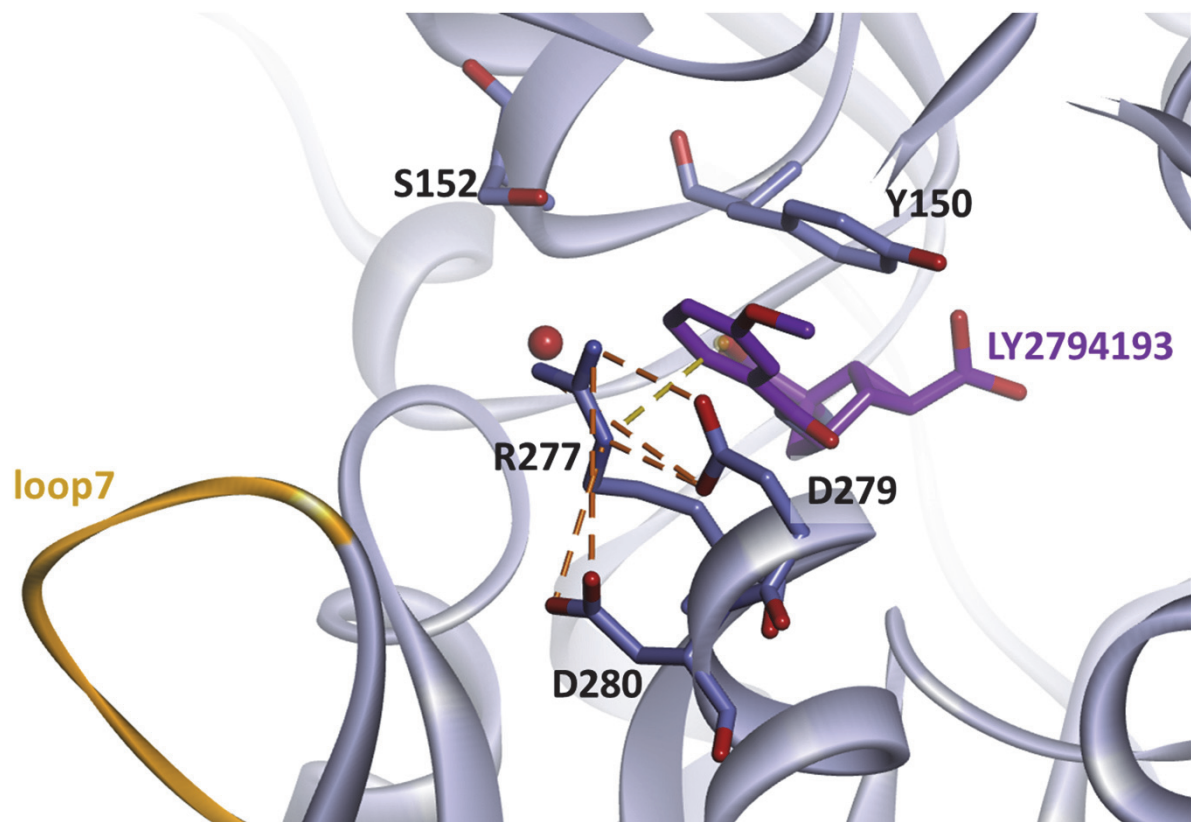
D



Supplemental figure 6: Molecular determinants of mGlu3 chloride lock

A. Sequence alignment of the 8 mGluRs performed using Align123 on Discovery Studio suite and then optimized. Sequences were retrieved from Uniprot database (identifiers reported on the figure, middle column) and only the ECD parts were used (residue interval in right column). Numbers correspond to mGlu3R residue numbering. Blue color intensity is correlated by residue identity (dark), high similarity (medium) or low similarity (light). Key position in Cl⁻ binding are indicated in red (site 1) and yellow (site 2). mGlu2/3R cation-pi interlobe connection amino-acids are in orange. Loop intervals indicated with black double arrows. B. Bar plot of mGlu3 mutants pEC₅₀ values determined by TR-FRET mGlu sensor assay in high-Cl (open) and low-Cl (hatched) media. C. Calcium mobilisation assay of mGlu3 receptor mutants in high-Cl medium. Data are normalized by TR-FRET largest window defined by top and bottom of the mGlu3 WT dose-response curve in low-Cl. D. Expression of HA SNAP and HA mGlu3 constructs as determined by ELISA. Open bar: cell surface expression; hatched bar: total expression. All constructs dose-response parameters are listed in supplemental table 2. Glu: glutamate. VEH: vehicle.

Supplemental figure 7



Supplemental figure 7: LY2794193, selective mGlu3 agonist bound to mGlu3 binding site (Monn et al 2018)

The phenyl substituent of LY2794193 pushes R277 but keeping a cation-II interaction instead of with Y150. The curled loop 7 (brown) that stabilizes the active dimer is maintained and activation of mGlu3 occurs. At mGlu2, the analogous R271 is pushed similarly but the disruption of its bindings seems to prevent the stabilization of the active conformation of the receptor. Consequently, mGlu2 activation is notably decreased.

SUPPLEMENTAL TABLES

Supplemental table 1

IP1				
Receptor	Agonist	pEC ₅₀ (EC ₅₀ μM)	Base (%)	N
mGlu ₃ WT		-	38,76 ± 3,00	3
mGlu ₂ WT	Glutamate	4,79 ± 0,07 (16,22)	100,00 ± 0,00	3
VFT2/TMD3		4,56 ± 0,08 (27,54)	148,47 ± 12,48	3
VFT3/TMD2		-	41,69 ± 4,57	3

TR-FRET sensor				
Receptor	Agonist	pEC ₅₀ (EC ₅₀ μM)	Base (%)	N
mGlu ₃ WT		5,30 ± 0,14 (5,01)	15,22 ± 3,01	3
mGlu ₂ WT	Glutamate	4,99 ± 0,13 (10,23)	100,00 ± 0,00	3
VFT2/TMD3		4,71 ± 0,16 (19,50)	111,27 ± 1,19	3
VFT3/TMD2		6,06 ± 0,08 (0,87)	7,84 ± 2,22	3

Supplemental table 1: Concentration-response curves parameters of mGlu₂-mGlu₃ chimeras.

Potency (pEC₅₀) and basal response (vehicle stimulation) of TR-FRET sensors and IP1 curves are derived from data normalized by mGlu2 WT window (top and bottom of mGlu2 curve). Parameters values represent the mean ± SEM from three experiments (N) performed in triplicates.

- : Not Determined

Supplemental table 2

Receptor	Agonist	High Cl ⁻ buffer			Low Cl ⁻ buffer			N	Chloride sensitivity
		pEC ₅₀ (EC ₅₀ μM)	E _{max} (%WT)	nH	pEC ₅₀ (EC ₅₀ μM)	E _{max} (%WT)	nH	ΔpEC ₅₀ (EC ₅₀ fold)	
Calcium mobilization									
mGlu ₃				5,27 ± 0,12					
WT		-	-	(5,37)		97,99 ± 2,66	2,00 ± 0,28	7	-
mGlu ₃	Glutamate	6,10 ± 0,30 (0,79)	125,44 ± 4,16	1,97 ± 0,51	4,73 ± 0,06 (18,62)	119,83 ± 7,94	2,51 ± 0,41	5	-1,37 ± 0,31 (23,44)
mGlu ₃		6,56 ± 0,13 (0,28)	119,68 ± 5,80	1,18 ± 0,16	6,14 ± 0,04 (0,72)	107,18 ± 2,14	1,46 ± 0,24	5	-0,44 ± 0,11 (2,75)
S152D									
TR-FRET sensor									
mGlu ₃		pEC ₅₀ (EC ₅₀ μM)	Base (%WT)	nH	pEC ₅₀ (EC ₅₀ μM)	Base (%WT)	nH		ΔpEC ₅₀ (EC ₅₀ fold)
WT		5,62 ± 0,11 (2,40)	61,24 ± 6,86	1,24 ± 0,09	4,36 ± 0,09 (43,65)	99,98 ± 0,02	2,27 ± 0,23	11	-1,26 ± 0,07 (18,20)
		6,05 ± 0,10 (0,89)	99,57 ± 2,10	0,71 ± 0,13					Extrapol.
mGlu ₃	Glutamate	5,22 ± 0,15 (6,03)	111,50 ± 12,81	1,94 ± 0,14	3,86 ± 0,07 (138,04)	147,13 ± 8,22	3,86 ± 0,07	6	-1,36 ± 0,15 (22,91)
mGlu ₃		5,30 ± 0,14 (5,01)	105,69 ± 12,34	1,88 ± 0,26	5,02 ± 0,11 (9,55)	109,77 ± 11,22	1,84 ± 0,32	6	-0,27 ± 0,05 (1,86)
mGlu ₃		-	-	-	-	-	-	3	-
T174A									
mGlu ₂		4,74 ± 0,19 (18,20)	95,61 ± 2,33	1,99 ± 0,26	4,14 ± 0,05 (72,44)	100,00 ± 0,00	1,41 ± 0,27	3	-0,60 ± 0,15 (3,98)

Supplemental table 2: mGlu₃ and mGlu₂ constructs concentration-response curves parameters in high Cl⁻ and low Cl⁻ buffers.

Potency (pEC_{50}), maximum response (E_{max}), basal response (vehicle stimulation) and Hill slope from concentration-response curves obtained with calcium mobilization and TR-FRET sensor assays. Values in red represent the extrapolated parameters from the TR-FRET glutamate concentration-response curve in high Cl⁻ without basal activity. Data are normalized by the maximum or basal response of the WT receptor in low Cl⁻ buffer. Parameters values represent the mean \pm SEM from at least three experiments (N) performed at least in duplicates. ΔpEC_{50} represent the loss of agonist potency due to chloride depletion.

- : Not Determined.